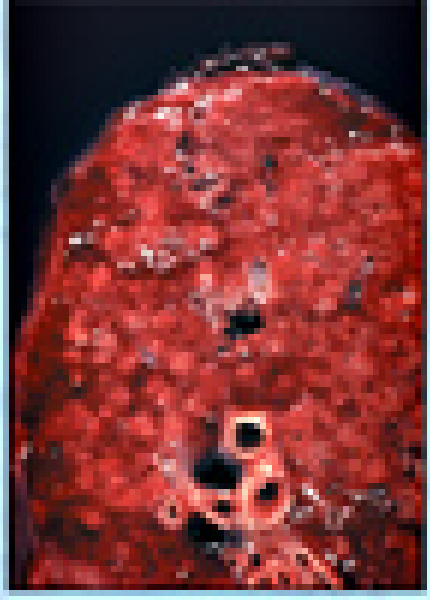

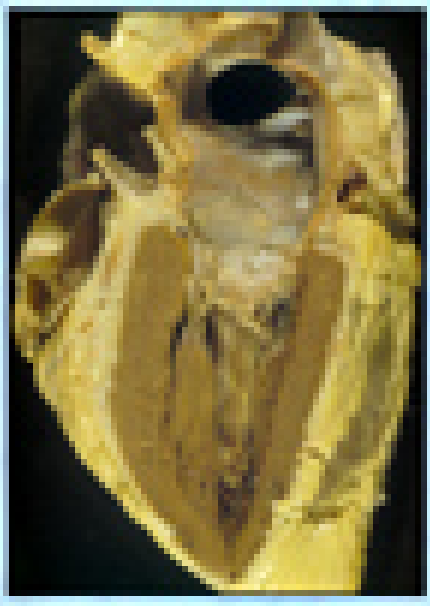

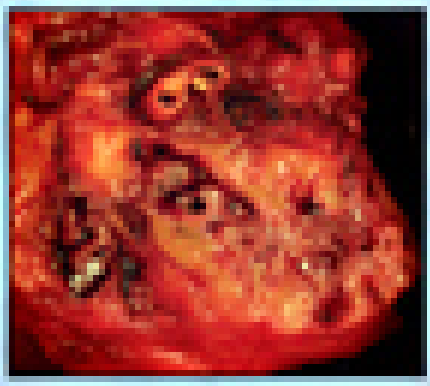

Atlas of Gross Pathology

with Histologic Correlation

ALAN G. ROSE

CAMBRIDGE Medicine

CAMBRIDGE www.cambridge.org/9780521868792

This page intentionally left blank

ATLAS OF GROSS PATHOLOGY

Detailed understanding of gross pathology is mandatory for successful pathologists, but this knowledge also provides a sound foundation for those intending to become surgeons, internists, and obstetrician/gynecologists. Some knowledge of gross pathology is important for members of the allied health professions and dental students. For pathologists, pathology residents, and pathology assistants, knowledge of gross pathology is essential for guidance in selecting the correct areas of pathologic lesions to sample for microscopy and frozen section examination. This atlas aims to provide a comprehensive illustration and description of a wide range and number of pathologic processes and diseases affecting all the major organs of the body. Emphasis is placed on how the anatomic structure of different organs may determine the pattern of involvement by disease processes and how such patterns may aid in the correct diagnosis of the gross pathology. In some cases, multiple illustrations of disease processes are given to show evolution of the disease. Histologic illustrations of selected gross lesions are also included where relevant. The atlas is illustrated with more than 1,200 color photographs.

Dr. Alan G. Rose, MD, FRCPath, FACC, is Professor of Pathology at the University of Minnesota Medical School. He is also the Director of Autopsy Service at the University of Minnesota Medical Center, Fairview; the Residency and Fellowship Training Program; and the Medical School Pathology Teaching Program at the University of Minnesota.

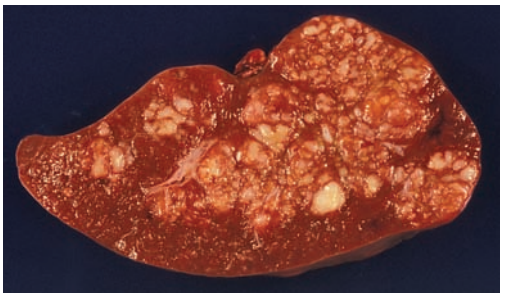

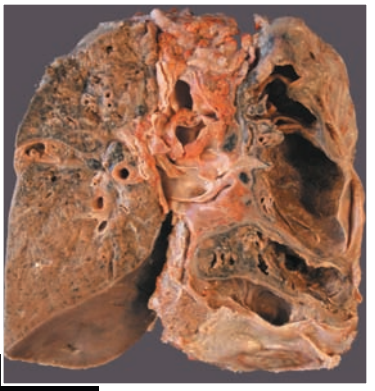

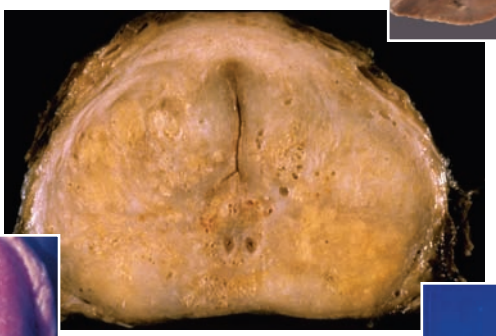

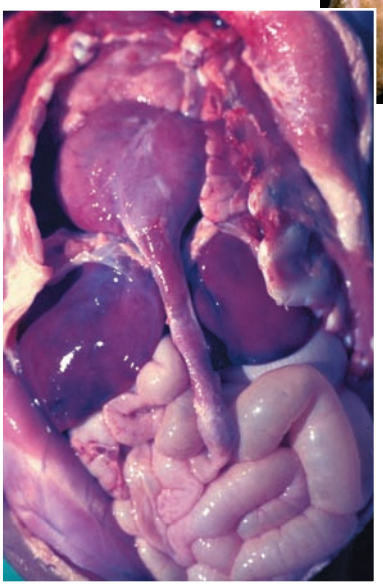

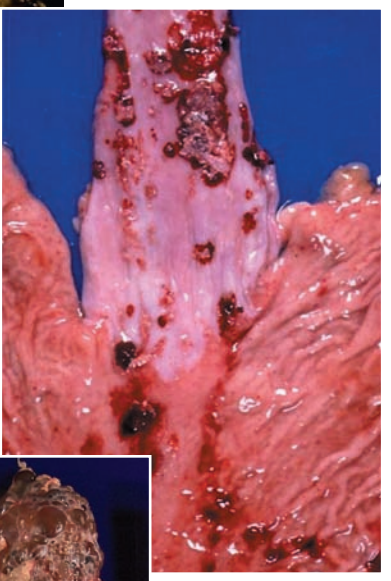

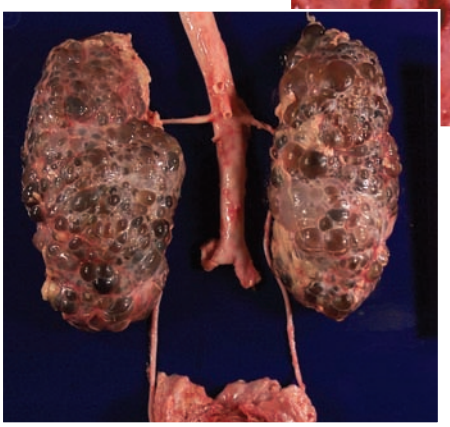

ATLAS OF GROSS PATHOLOGY

with Histologic Correlation

ALAN G. ROSE
University of Minnesota

CAMBRIDGE
UNIVERSITY PRESS

CAMBRIDGE UNIVERSITY PRESS
Cambridge, New York, Melbourne, Madrid, Cape Town, Singapore, São Paulo

Cambridge University Press
The Edinburgh Building, Cambridge CB2 8RU, UK
Published in the United States of America by Cambridge University Press, New York

www.cambridge.org
Information on this title: www.cambridge.org/9780521868792

First published in print format 2008

ISBN-13 978-0-511-43382-5 eBook (Adobe Reader)

ISBN-13 978-0-521-86879-2 hardback

CONTENTS

ATLAS OF GROSS PATHOLOGY

1 Cardiac Diseases

CONGENITAL DISEASES

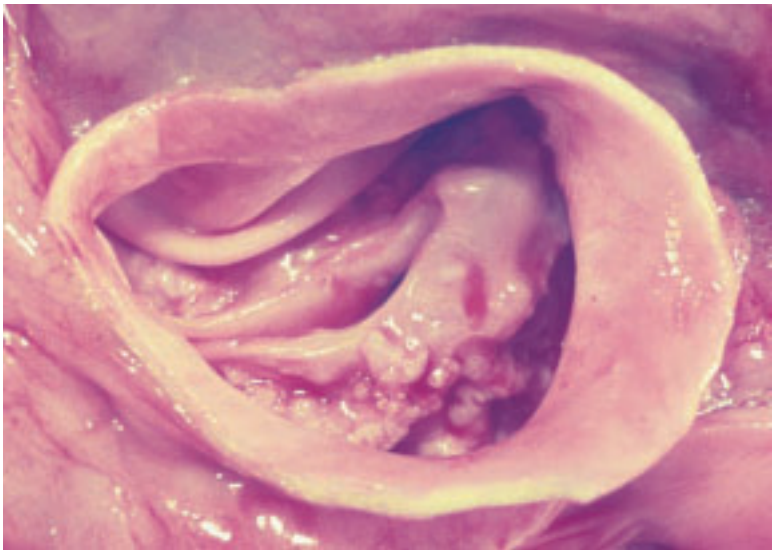

1-1. Unicuspid unicommissural aortic valve has become stenotic in middle age due to calcification of the abnormally stressed single cusp.

1-2. Congenital aortic stenosis due to a bicuspid aortic valve with thick, dysplastic cusps. Each cusp is approximately the same length as the other (i.e., stenosis occurs because no abnormally long conjoined cusp is present).

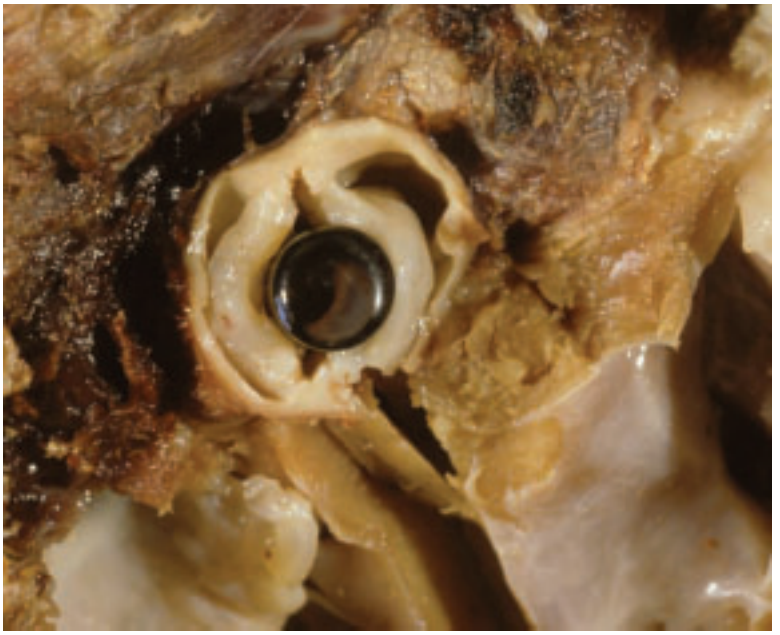

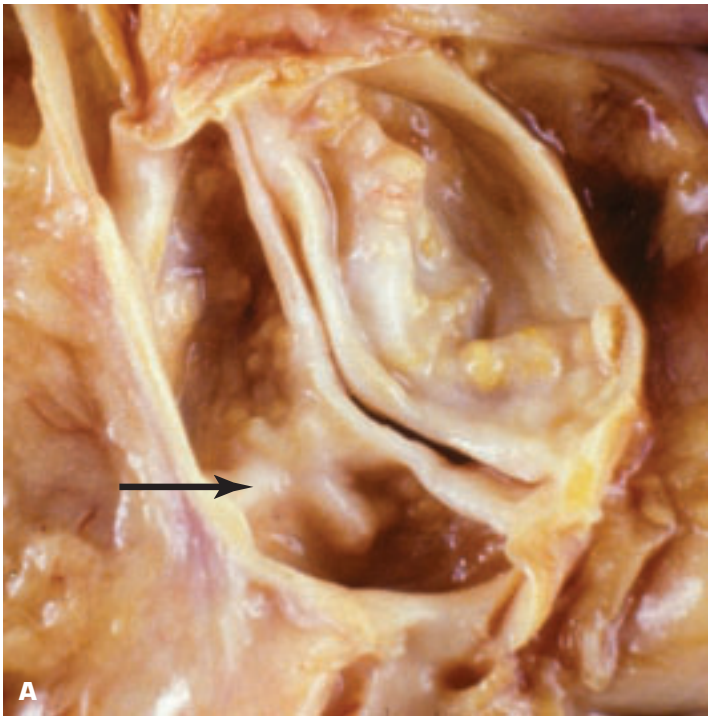

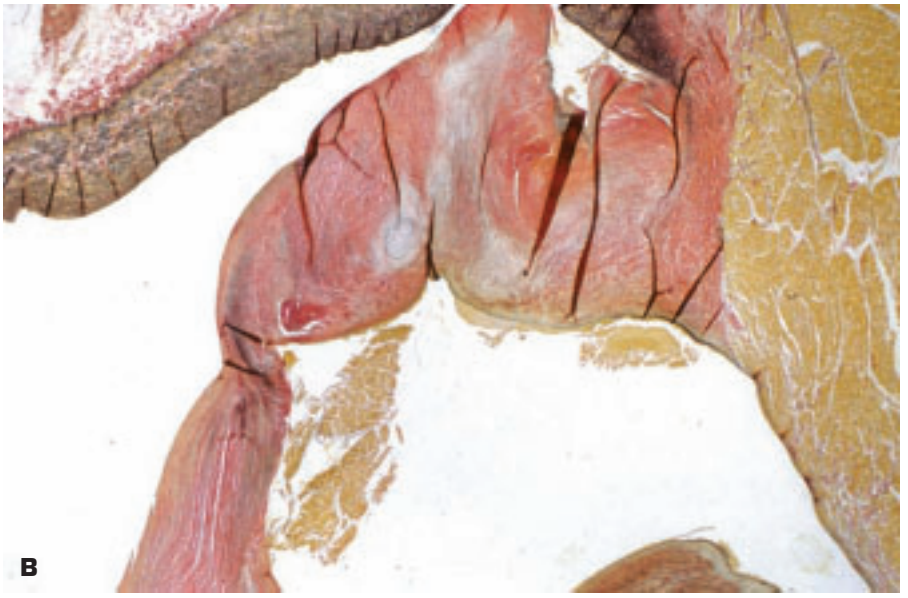

1-3. A. Aortic stenosis due to calcified congenital bicuspid aortic valve in a 50-year-old man. The longer conjoined cusp on the left is characterized by the presence of a raphe (*arrow*) that does not reach up to the free margin of the cusp. **B.** Microscopic section through the raphe shows fibrous tissue and no evidence of two preexisting separate aortic cusps (that may have fused).

1-4. Infective endocarditis affecting a bicuspid aortic valve in a patient who also has a small perimembranous ventricular septal defect situated immediately below the valve.

1-5. Congenital pulmonary stenosis: a small central hole is present at the top of a tent-like dome of fibrous tissue. The presence of four commissures gives an appearance suggesting four cusps are fused in forming this obstructing fibrous dome.

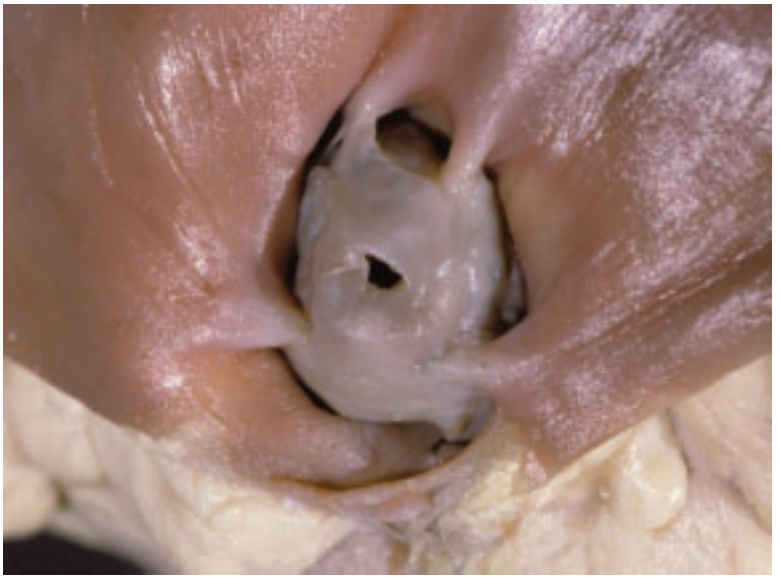

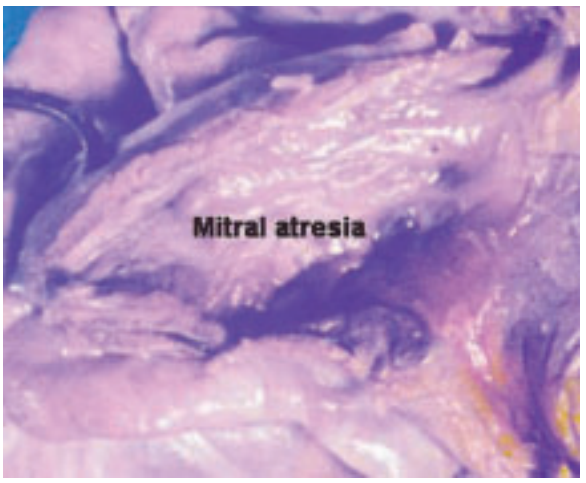

1-6. Congenital mitral atresia: no mitral valve is present, and there is only a central shallow dimple in the fibrous tissue occupying the space where the mitral valve should have been formed.

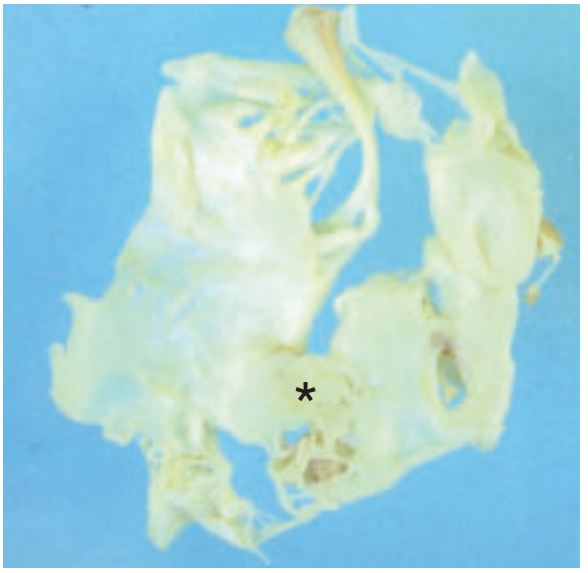

1-7. Appearance of a surgically excised mitral valve with double mitral orifice. The orifice of the valve is subdivided by a mass of abnormal valvular tissue (*) linking the two cusps.

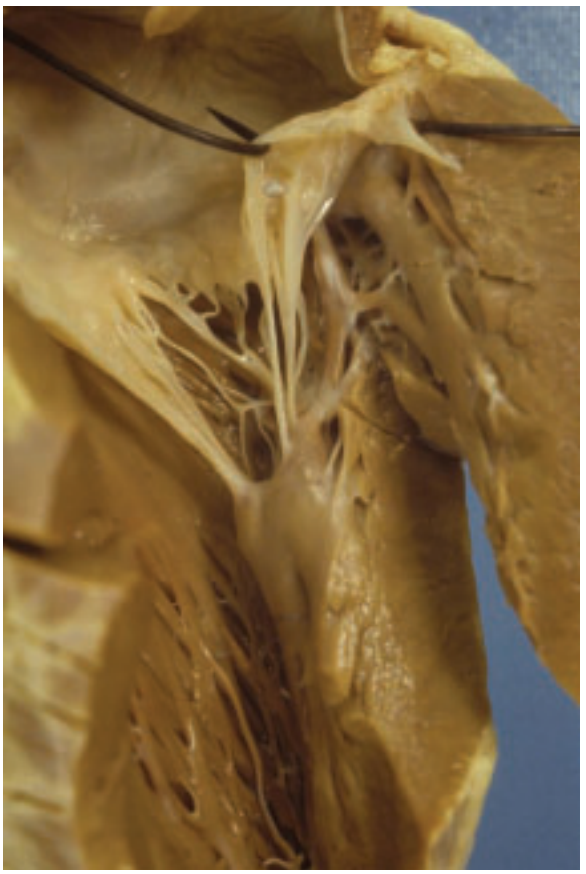

1-8. Parachute mitral valve, which may be functionally stenotic, is characterized by all of the chordae tendineae of the mitral valve being attached to a single papillary muscle. The diagnosis may easily be missed if the other missing papillary muscle is not noted.

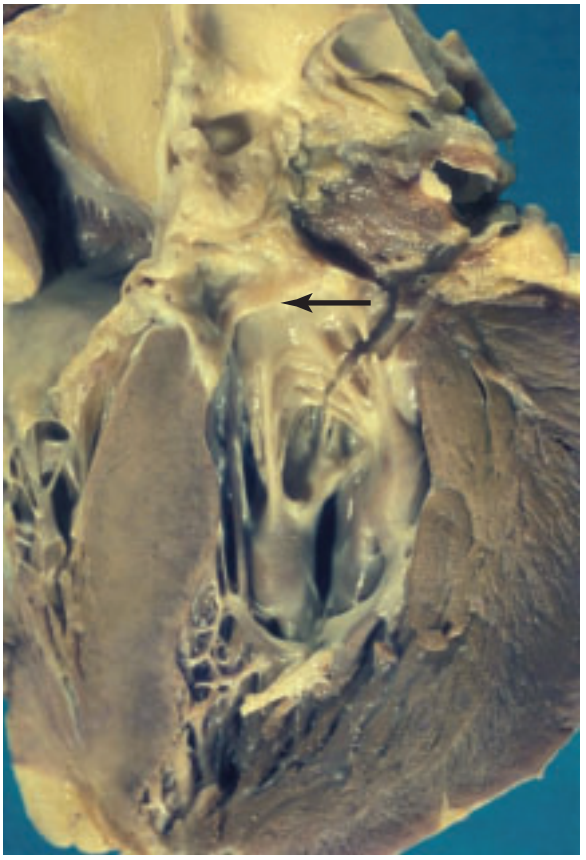

1-9. Recurrent subaortic membranous stenosis (*arrow*) after prior resection of an obstructing fibrous membrane running across the muscular ventricular septum and the anterior mitral leaflet. The membrane may re-form repeatedly after resection in some individuals. The aortic valve is thickened and deformed secondary to the effects of the subaortic obstruction-induced jet lesion.

1-10. Ebstein's anomaly of the tricuspid valve showing atrialization of the proximal portion of the right ventricle due to downward displacement of the tricuspid valve ring. The very large, dysplastic tricuspid valve is also plastered down against the underlying right ventricular endocardium in multiple areas, rendering the valve incompetent.

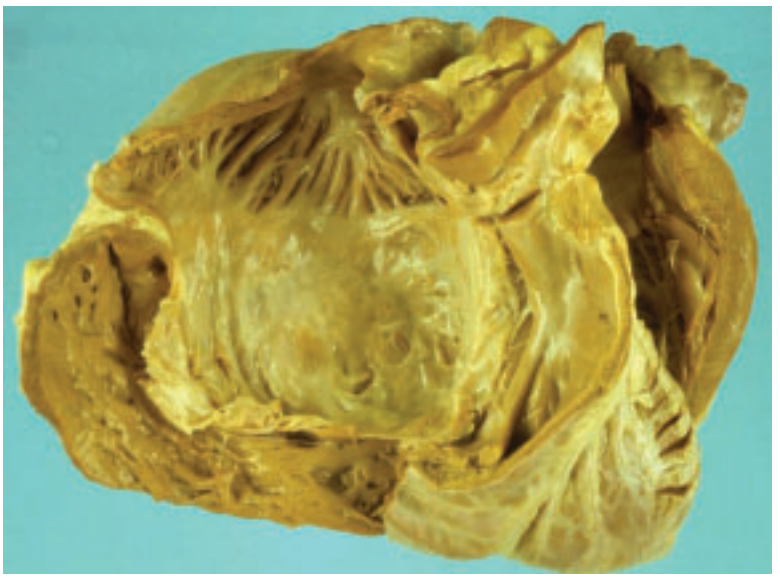

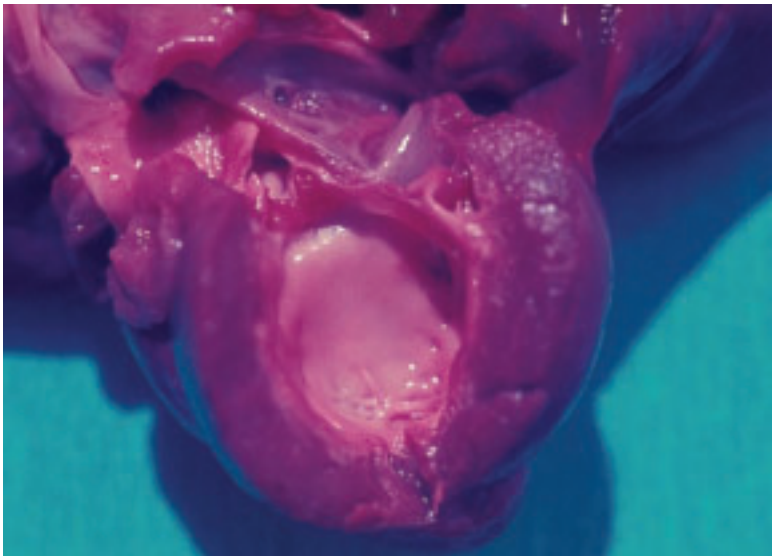

1-11. Endocardial fibroelastosis: the left ventricle is lined by a porcelain-like layer of fibrous tissue. Some patients give a history of maternal mumps infection during pregnancy.

1-12. Probe indicates a patent foramen ovale, and a small red thrombus is adherent to the nearby margin of the fossa ovalis (*right*). Transvenous atrial closure devices have been developed to seal such defects and thus prevent passage of thrombus via the patency to reach the left atrium.

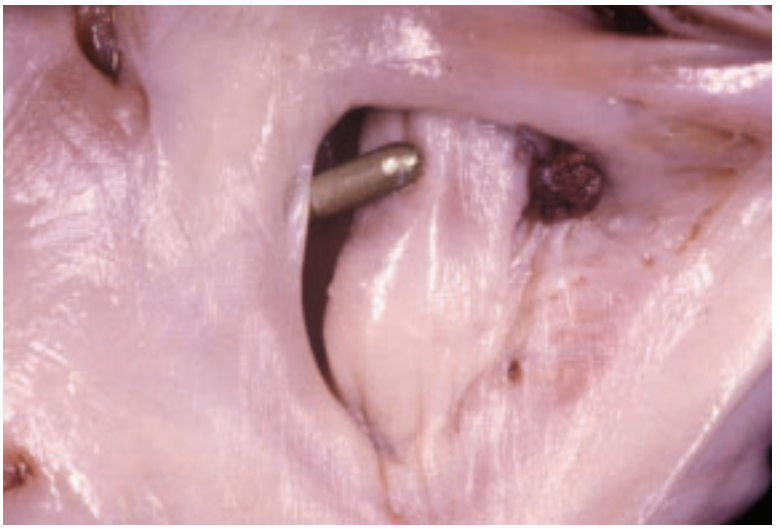

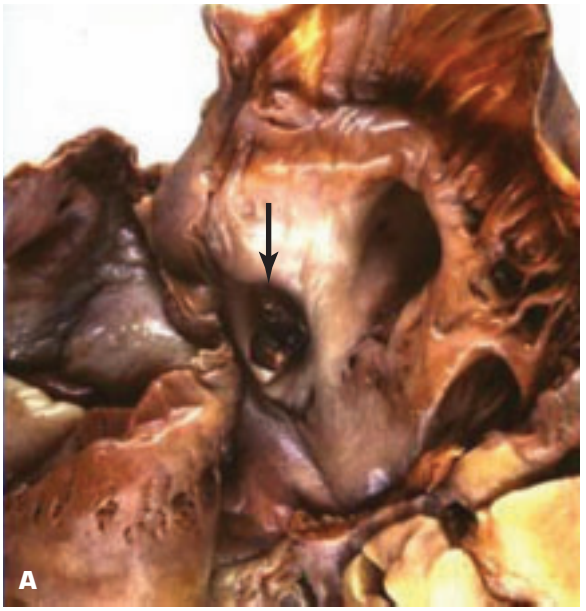

1-13. A paradoxical embolus occurs when a thrombus passes from the right atrium into the left atrium and then into the systemic circulation producing arterial occlusion. **A.** View from right atrium of a paradoxical embolus (*arrow*) passing across a patent foramen ovale. **B.** Left atrial view of the other end of the thromboembolus (*arrow*) that is passing across the patent foramen ovale.

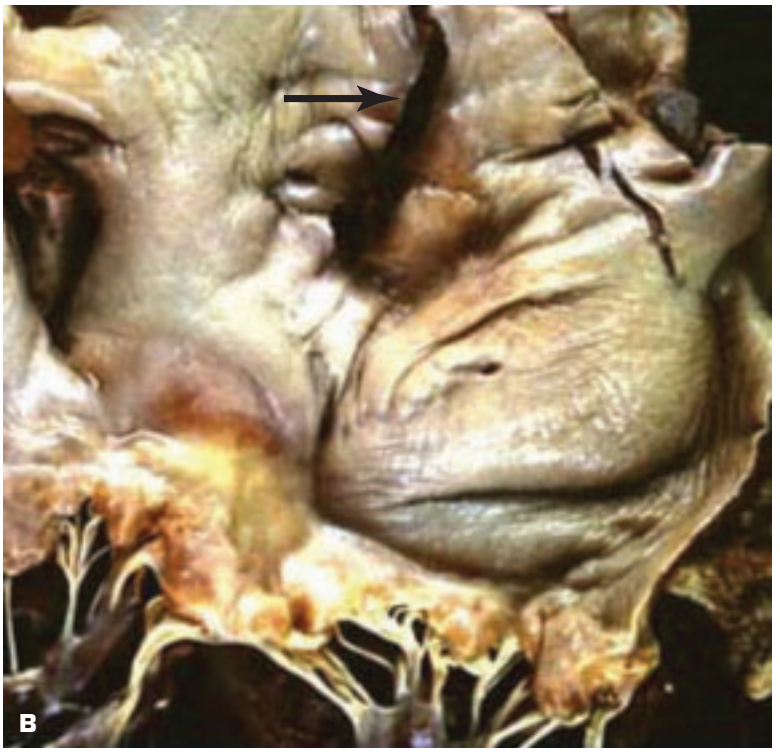

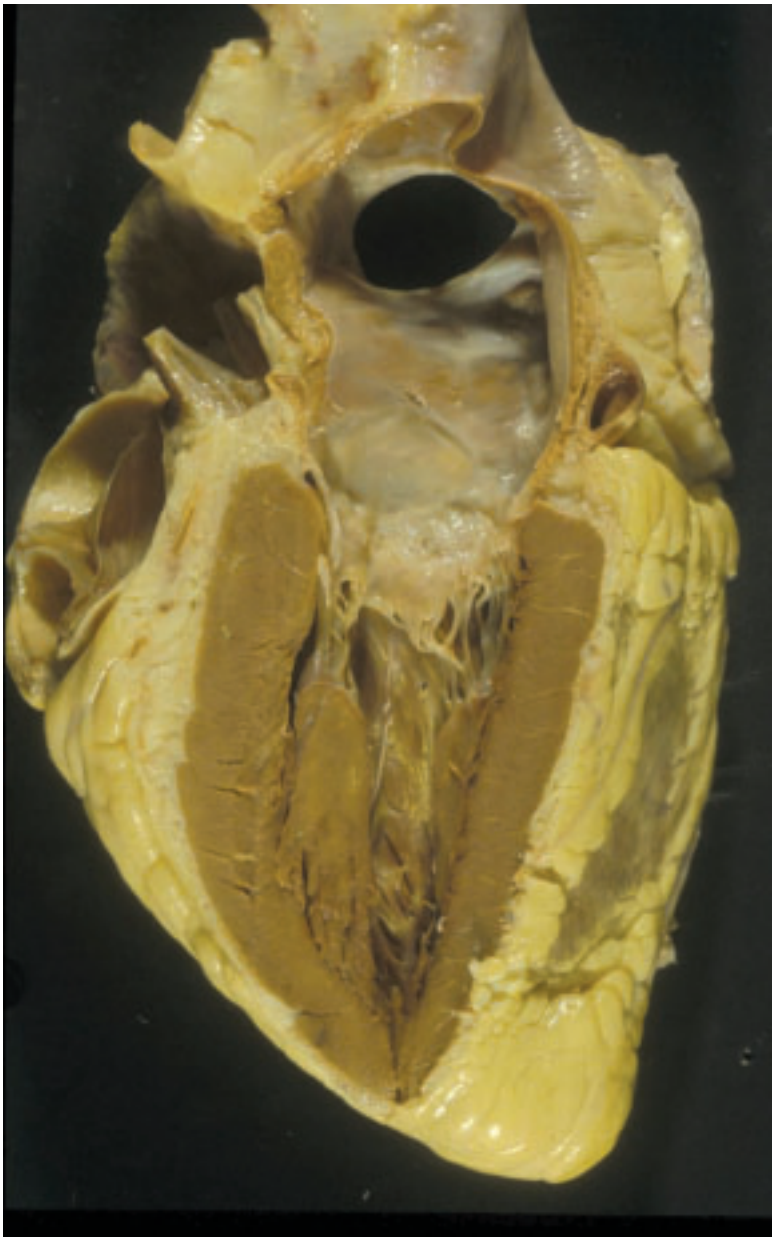

1-14. Secundum atrial septal defect at site usually occupied by the fossa ovalis in the interatrial septum.

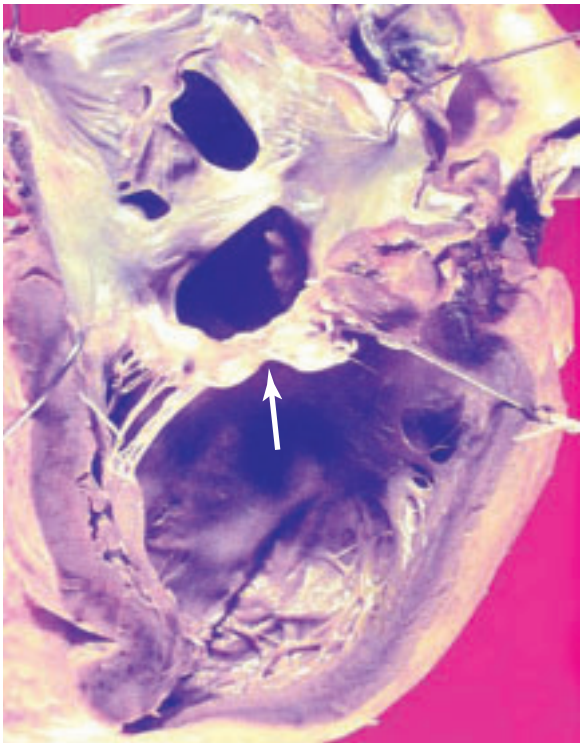

1-15. Ostium secundum (upper hole) and ostium primum (lower hole) defects seen on left side of the heart. The anterior cusp of the mitral valve has a cleft (*arrow*) in it as part of the ostium primum defect. This 48-year-old woman presented with pulmonary hypertension due to the long-standing left-to-right shunt at atrial level. She died while awaiting a heart-lung transplant.

1-16. Appearance of anterior leaflet of the mitral valve in ostium primum defect with two separate atrioventricular valves: multiple short tethering chordae limited the movement of the anterior mitral cusp during left ventricular systole. In addition to closing the defect with a patch, the surgeon needs to cut these abnormal chordae to allow normal mitral valve function.

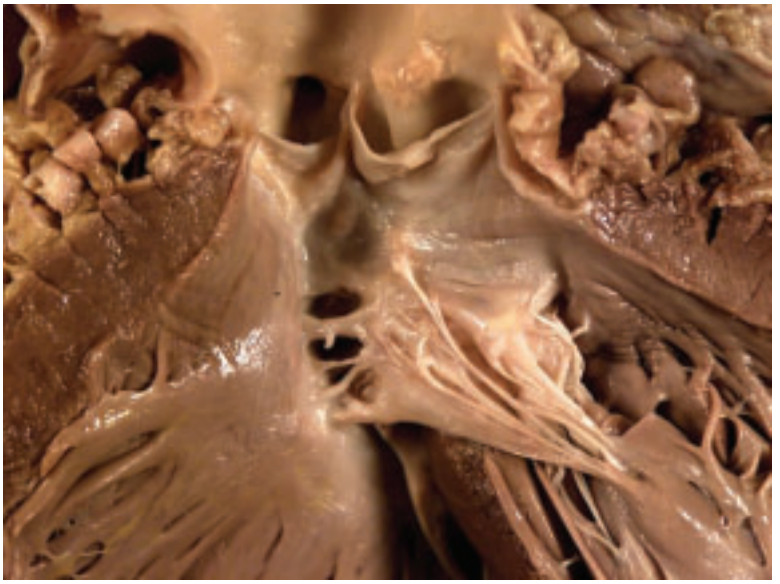

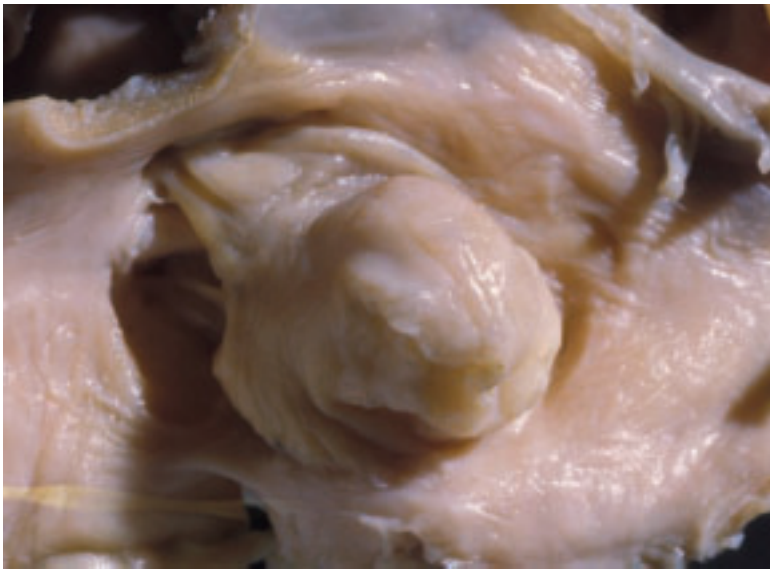

1-17. Aneurysm of the fossa ovalis (flap valve) may be a primary abnormality per se or may be associated with valvular disease (e.g., mitral valve atresia). The aneurysm always points into the lower pressure zone. Such aneurysms may also be acquired in later life.

1-18. Perimembranous ventricular septal defect: the hole includes the area of the membranous septum plus some surrounding muscular tissue.

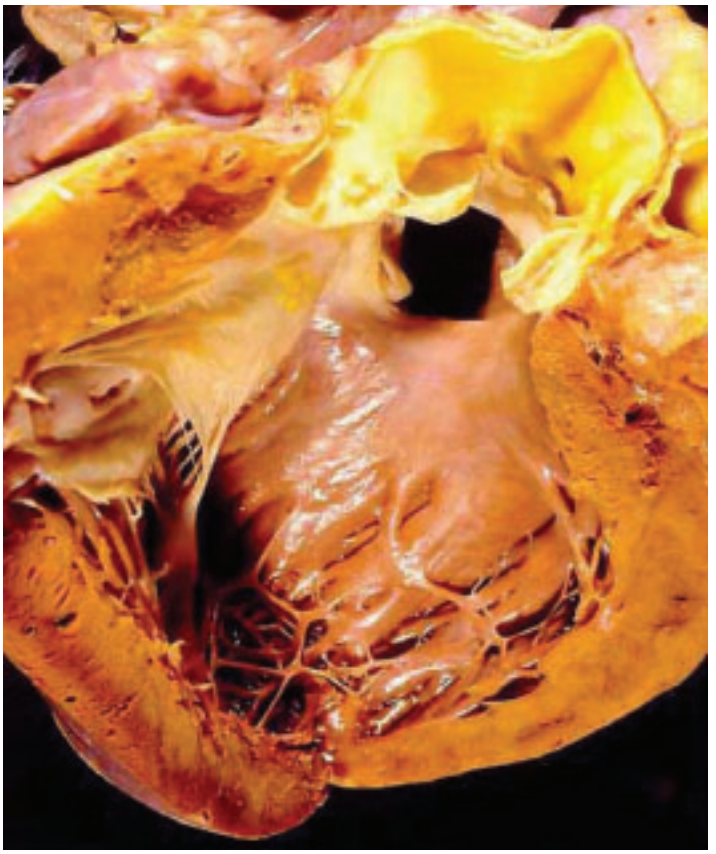

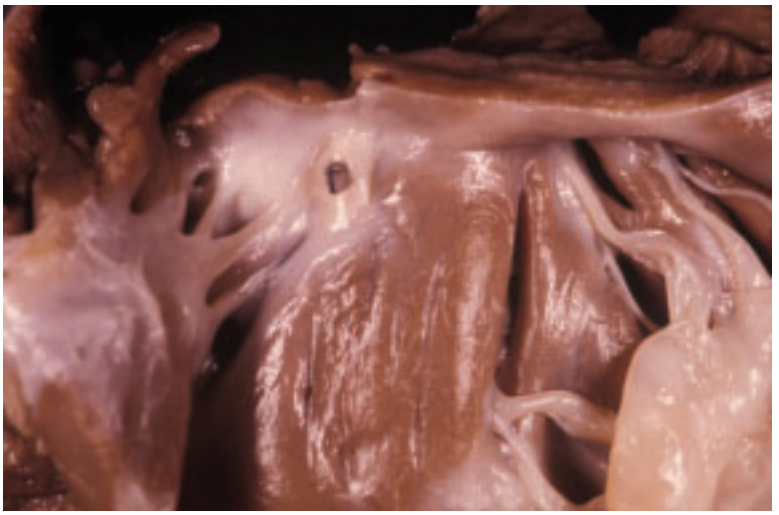

1-19. Right ventricular end of a small muscular ventricular septal defect shows surrounding endocardial fibrous thickening due to turbulent blood flow (jet lesion).

1-20. Top Dacron patch seals atrial septal defect and lower Dacron patch sealing ventricular septal defect (VSD) is the site of infection (infective endocarditis of VSD patch). The patch has been sampled for microbiology and histology.

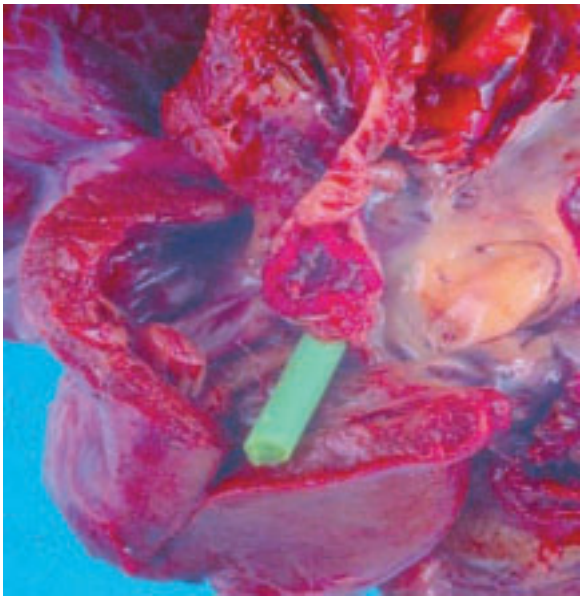

1-21. Postoperative tetralogy of Fallot showing dehiscence of Dacron patch sealing right side of an infracristal ventricular septal defect. A probe passes upward from the right ventricle behind the free margin of the patch to enter the left ventricle (not seen in this view).

1-22. Total anomalous pulmonary venous drainage: the confluence of the four pulmonary veins has no connection to the left atrium, but in this patient drained inferiorly below the diaphragm. Note that the apex of the heart has been displaced vertically to expose the major pulmonary veins.

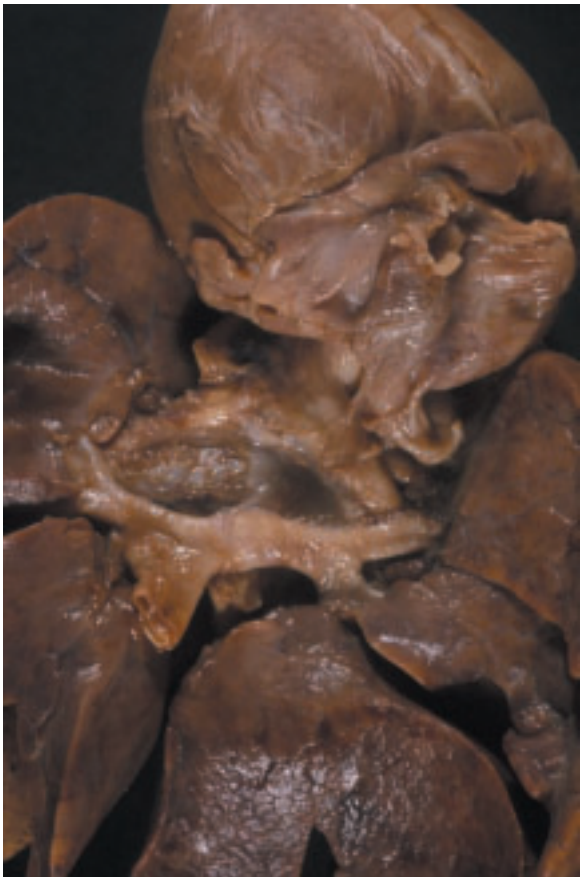

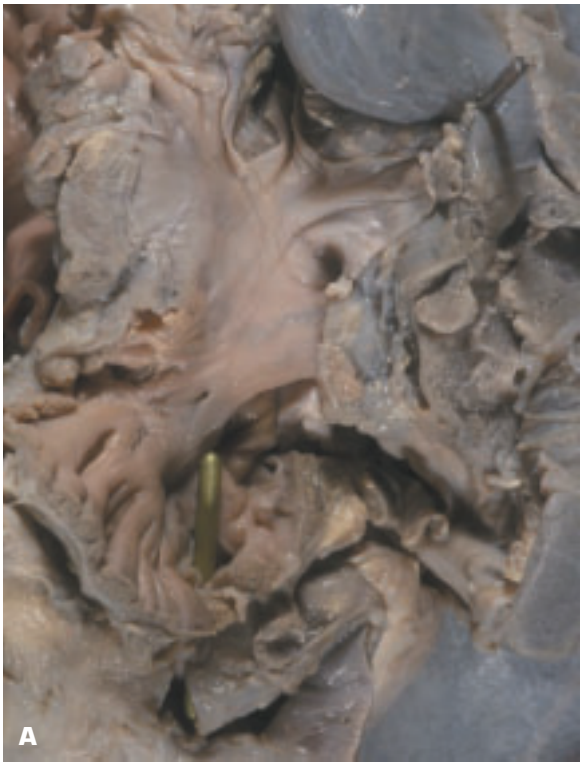

1-23. Cor triatriatum results from failure of incorporation of the common pulmonary vein into the left atrium during the fifth week of embryological development. A fibromuscular diaphragm subdivides the left atrium into two chambers linked by a small hole. **A.** Upper chamber with small hole in its floor (probe). **B.** Lower chamber that leads directly into mitral valve orifice.

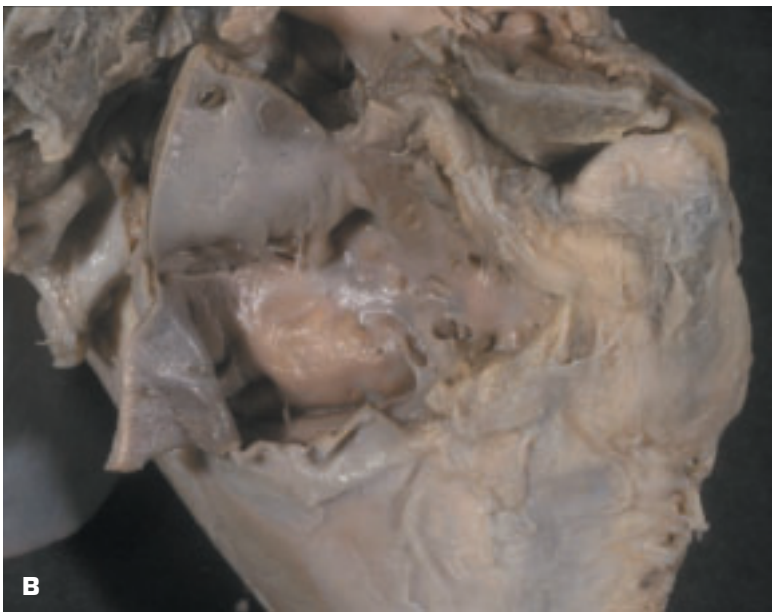

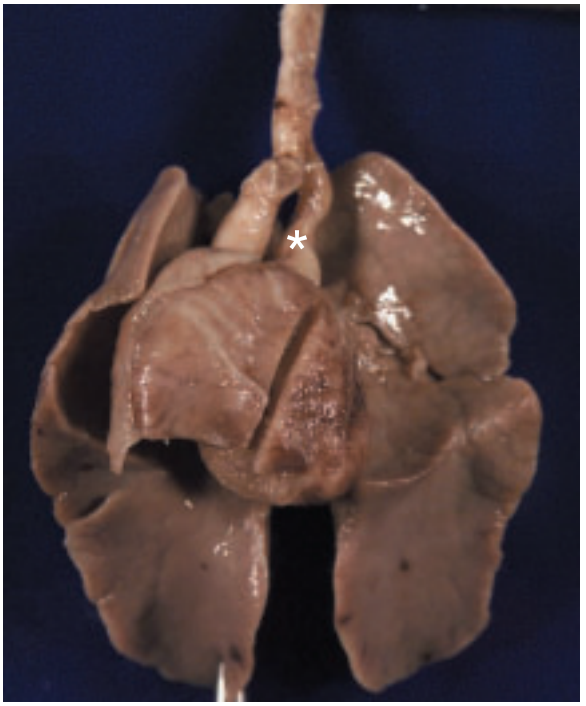

1-24. Patent ductus arteriosus (*) passes upward from pulmonary artery to join the aorta.

1-25. Surgically resected coarctation of the aorta has been bisected longitudinally to reveal a curtain-like fold of aortic tissue that affects the superior, anterior, and posterior portions of the aorta, but spares its inferior portion. One theory of causation attributes ectopic ductal tissue as the cause of the lesion.

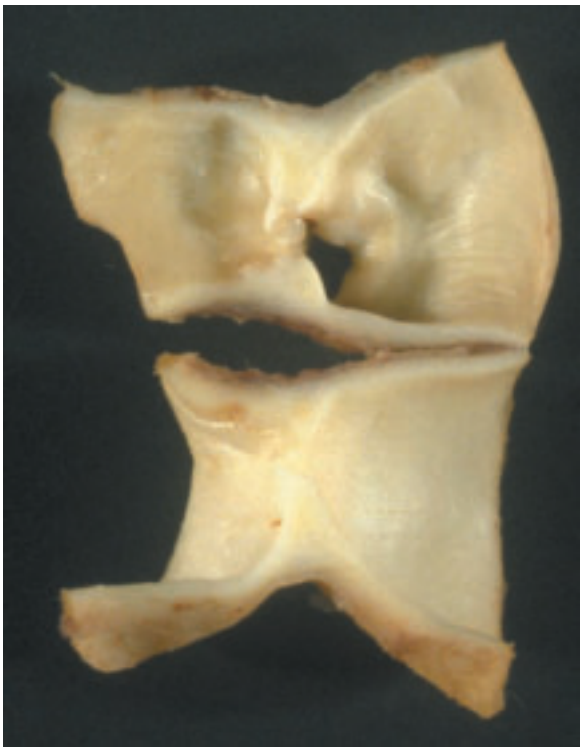

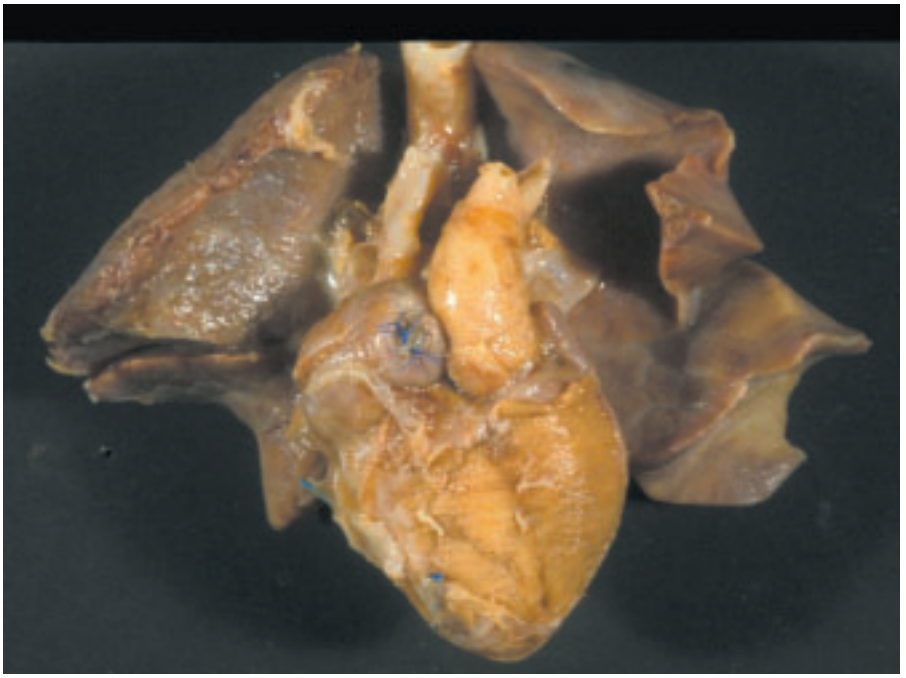

1-26. Transposition of the great arteries. The aorta (note the origins of the arch branches) is seen to be arising from the right ventricle at the expected origin of the pulmonary artery, and the latter (not visible in this view) arises from the left ventricle. The descending thoracic aorta had a left-sided descent.

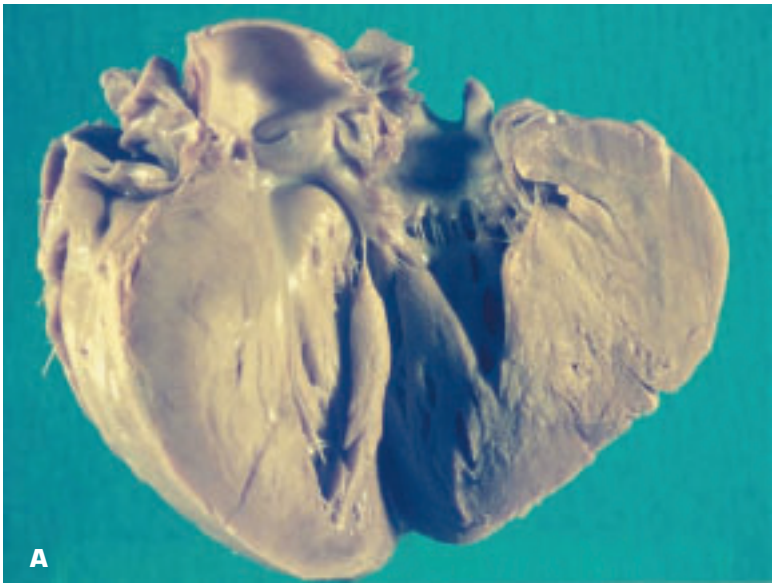

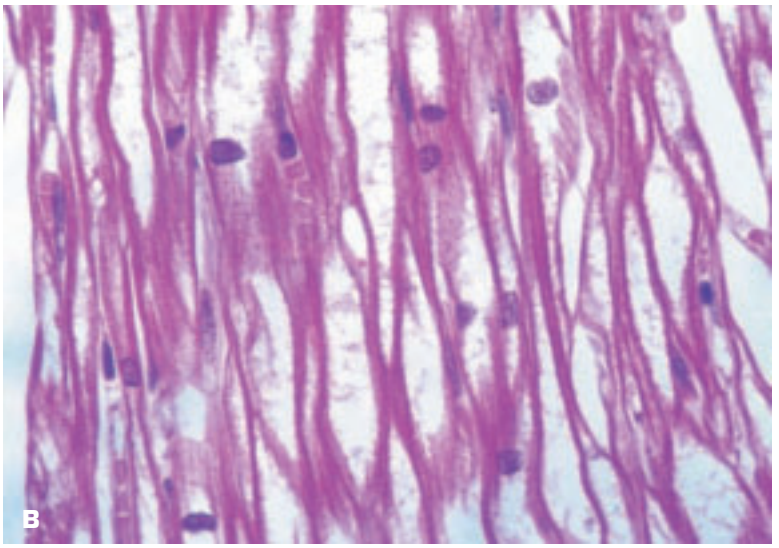

1-27. A. Glycogen storage disease has produced massive concentric hypertrophy of the cardiac chambers. **B.** Histology shows swollen, vacuolated myocytes due to massive accumulation of glycogen.

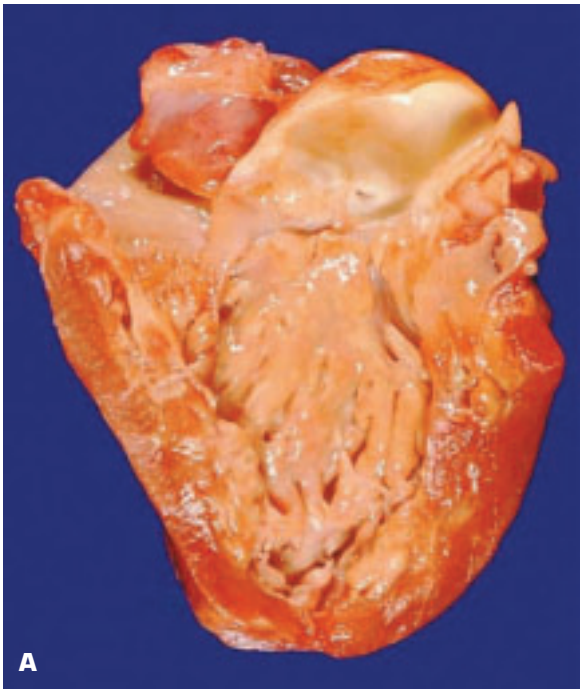

1-28. A. Bosselated appearance of left ventricular endocardium in histiocytoid cardiomyopathy. **B.** Histologic appearance of innermost portion of left ventricle showing vacuolated Purkinje fibers and myocytes expanding the subendocardium.

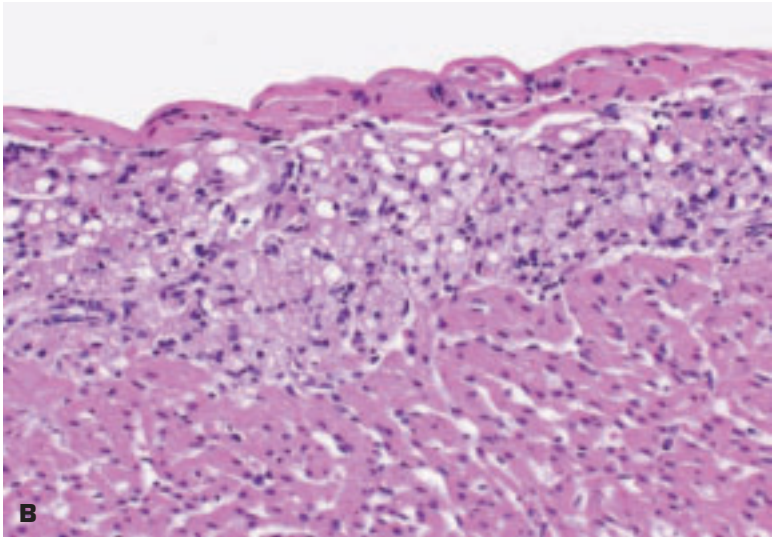

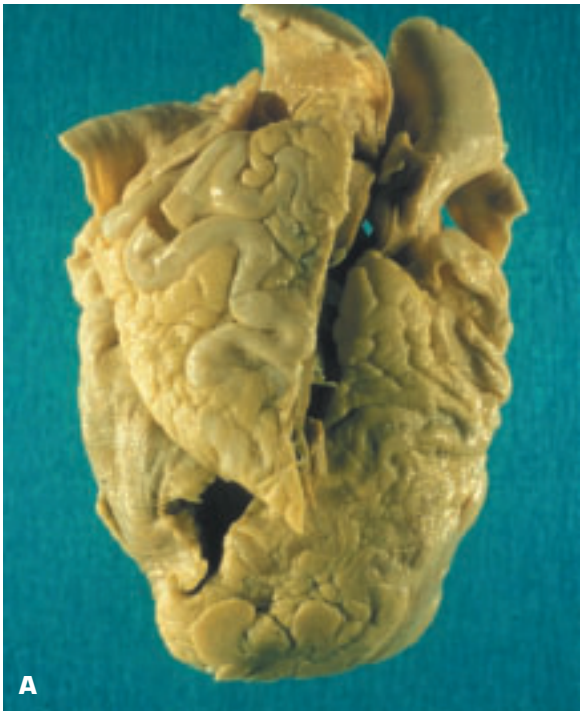

1-29. A. Biventricular coronary-cameral fistulae have led to marked ectasia and elongation of the major coronary arteries so that they resemble a "bag of worms" in appearance. The coronary arteries have had to carry much more blood than normal to compensate for blood lost into the cardiac chambers. **B.** Histologic appearance of left ventricle showing large arterial branches reaching to the endocardial zone.

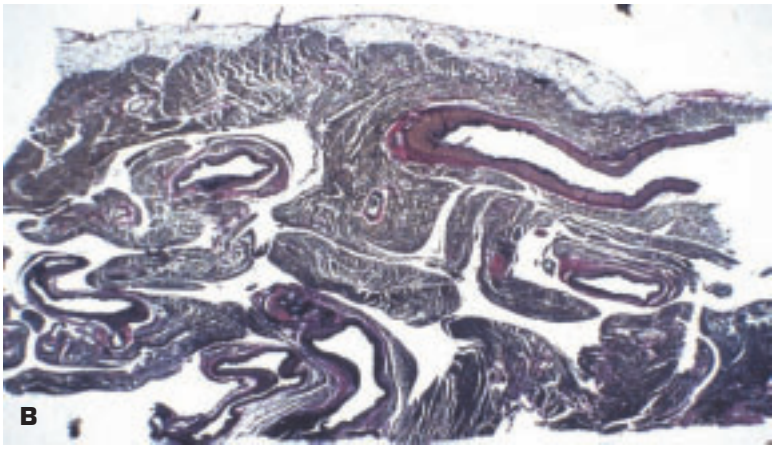

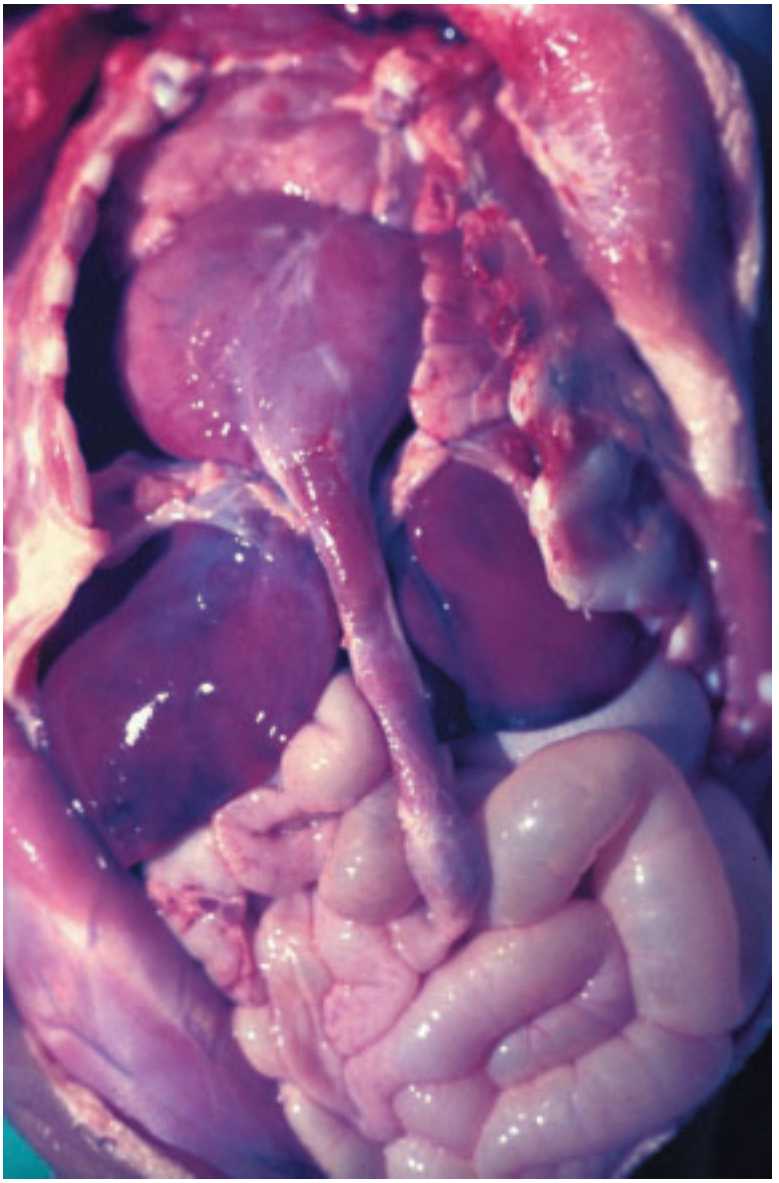

1-30. Congenital diverticulum arising from the apex of the left ventricle passed through the diaphragm anterior to the liver to terminate in the abdomen. Patient had pulsating umbilical swelling during life. Death was due to a hypoplastic left ventricle.

1-31. A. Senile calcific aortic stenosis due to calcium deposits in a tricuspid aortic valve that render the cusps relatively immobile. The deposits are mainly situated on the outflow aspect of all three cusps. **B.** Lipid deposits (central pale area) within the cusp that develop with age form the nidus for development of the calcification. **C.** Massive calcification expands the thickness of the cusp.

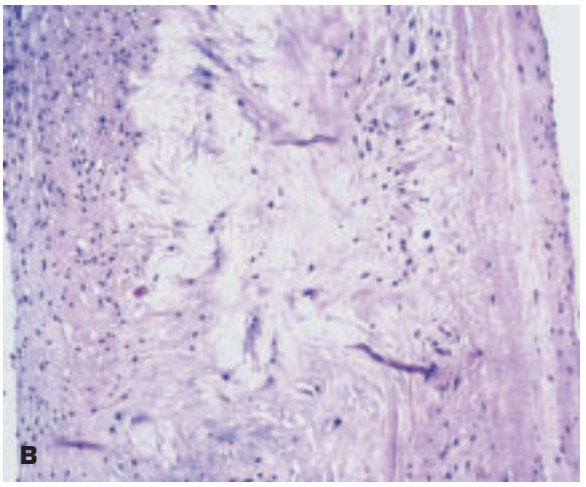

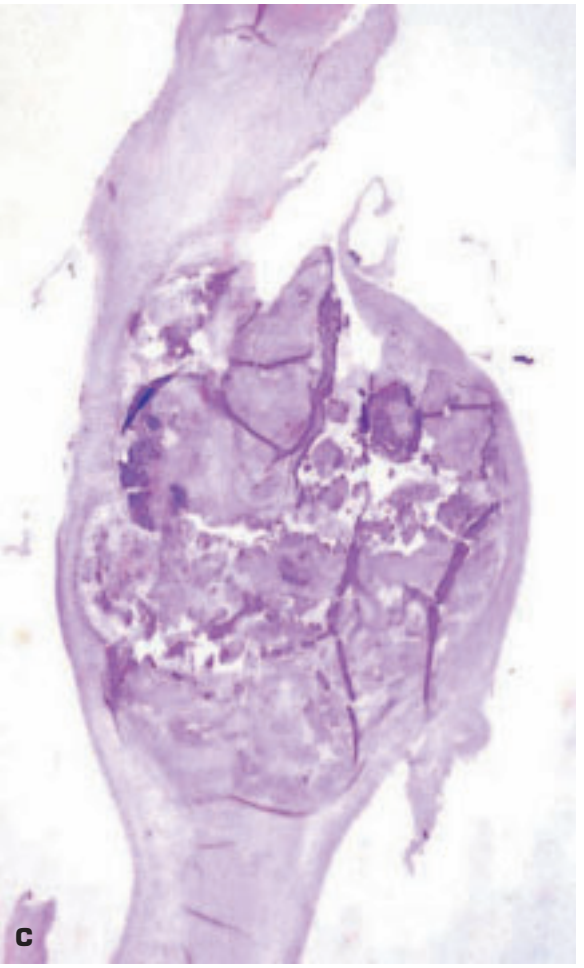

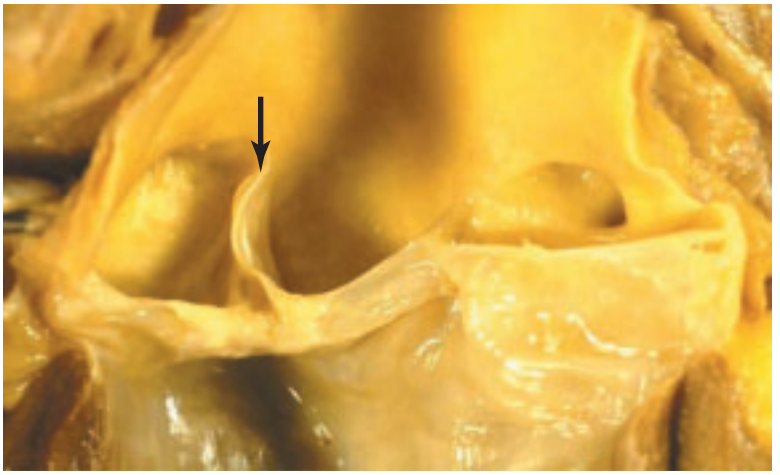

1-32. Acquired bicuspid aortic valve due to fusion (*arrow*) of one commissure. The fusion reaches right up to the free margin of the two united cusps and is unlike a raphe of a congenital bicuspid valve that would not reach up this high.

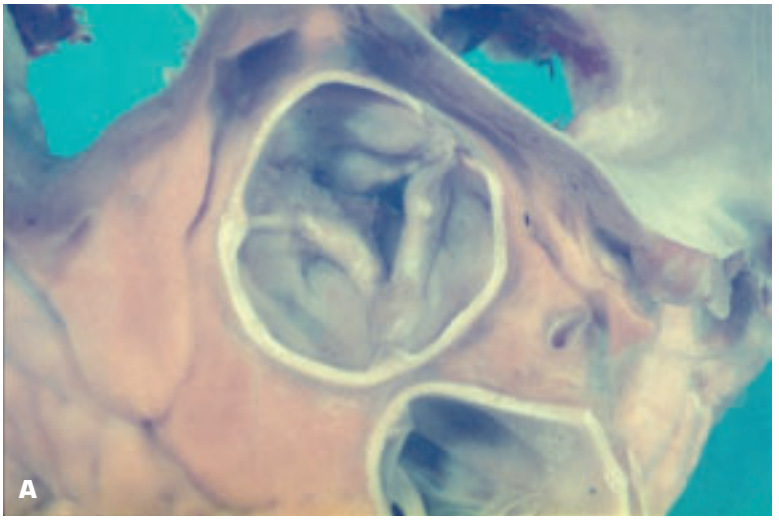

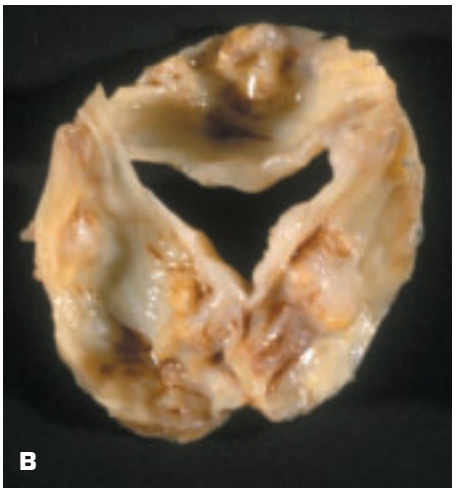

1-33. A. Acquired aortic stenosis due to rheumatic fever shows the typical triangular orifice due to partial fusion of all three commissures. Note also the thickness of the cusps. **B.** Surgically excised specimen of acquired aortic stenosis due to tricommissural fusion shows similar features.

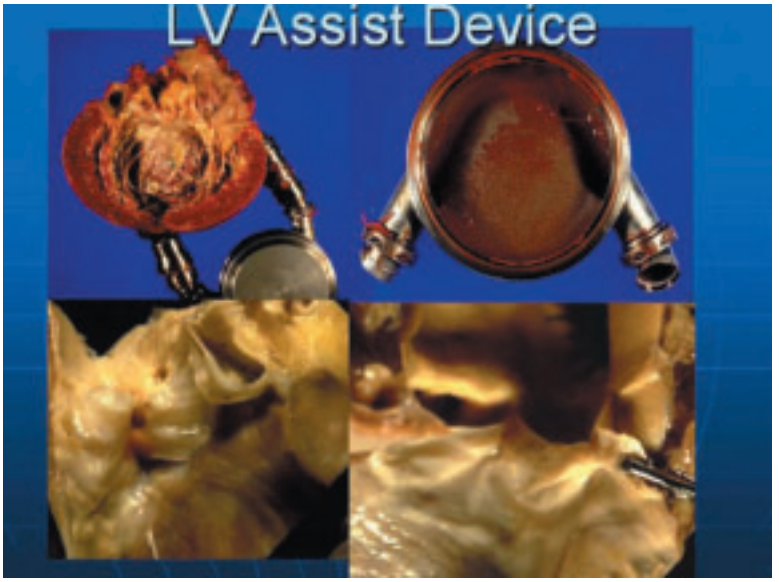

1-34. Acquired aortic stenosis in patients with left ventricular assist devices. For the assist pump to work well, the aortic valve stays permanently closed, favoring thrombosis and organization leading to commissural fusion. Left lower picture shows organizing thrombus on the inflow aspect of the aortic valve. Right lower picture shows commissural fusion leading to aortic stenosis.

1-35. Marantic endocarditis: note the large vegetations (thrombotic deposits) on the aortic valve in a patient with prior coronary arterial bypass grafts. Note hemoglobin staining of the aortic intima by intravascular hemolysis due to septicemia. Vegetations showed no sign of infection microscopically.

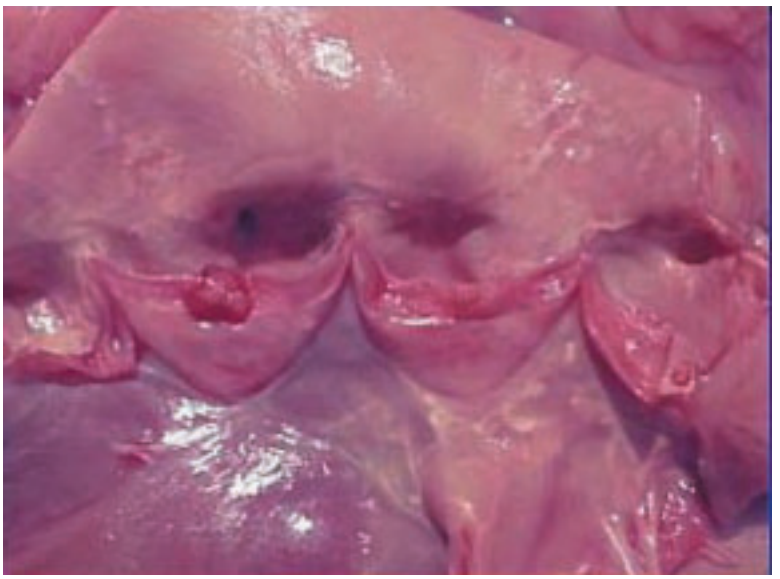

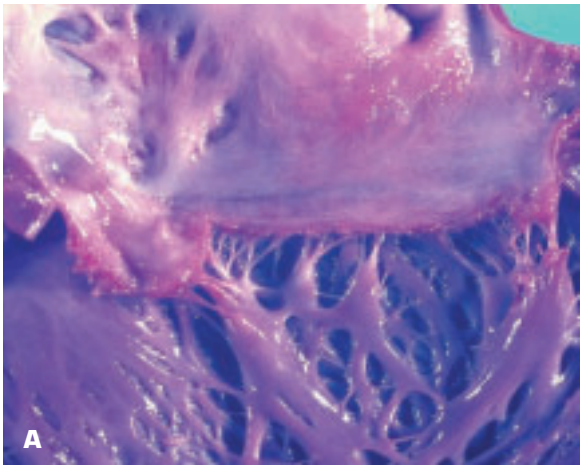

1-36. A. Small, firmly adherent, verrucous vegetations of acute rheumatic fever lie on contact area of the mitral valve cusps. Left atrium posterior wall has a MacCallum's patch (i.e., area of endocardial thickening due to the trauma of a regurgitant jet of blood from mitral incompetence). In acute rheumatic fever, increased numbers of Aschoff bodies may be found at this site of mechanical injury. **B.** Histology of rheumatic vegetation showing an Aschoff body with overlying fibrin deposition. **C.** Two Aschoff bodies in the proliferative phase lie on either side of a small intramyocardial coronary artery.

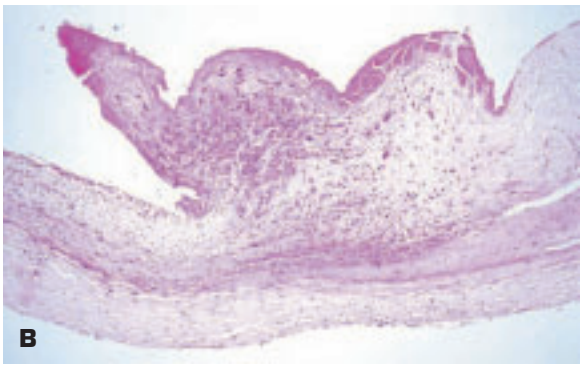

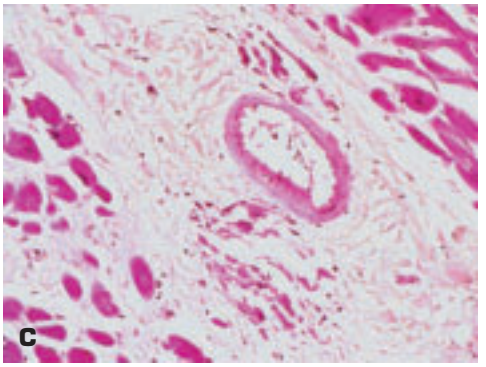

1-37. Tight mitral stenosis with a fish mouth orifice due to repeated attacks of acute rheumatic fever.

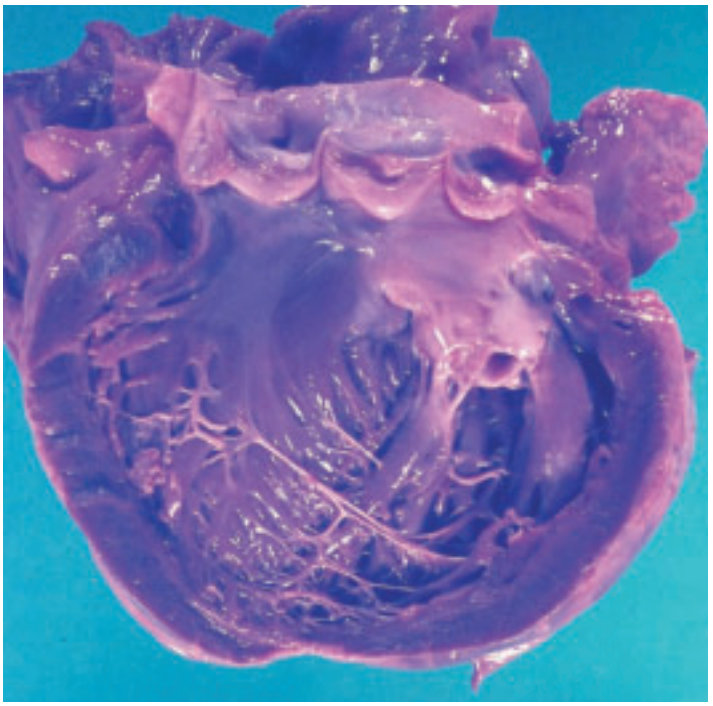

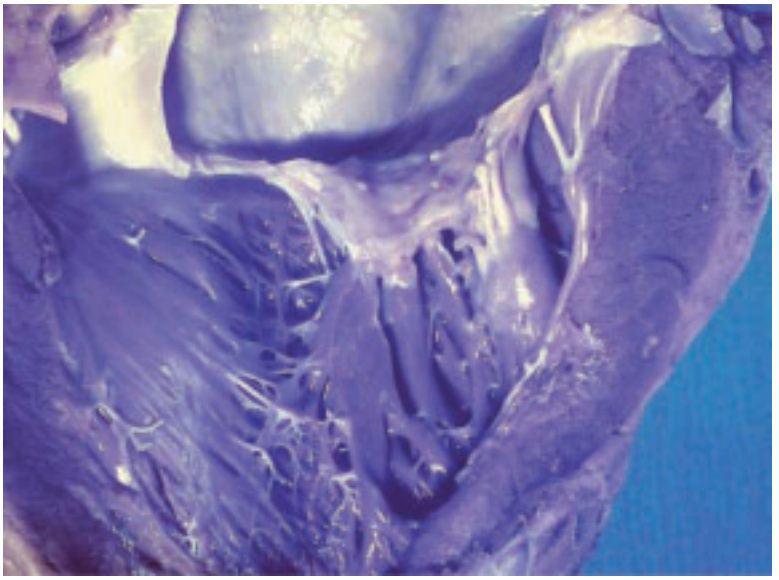

1-38. Severe postrheumatic mitral stenosis showing thickened, shortened cusps; fused commissures; and fused chordae tendineae.

1-39. Surgically excised mitral stenosis due to calcification at one commissure. The presence of the calcification (yellow-brown, ulcerated-looking area on the right) prevents the use of valvotomy to treat the stenosis. The calcification should not be mistaken for infective endocarditis. Infection rarely affects mitral stenosis and is more common in mitral regurgitation.

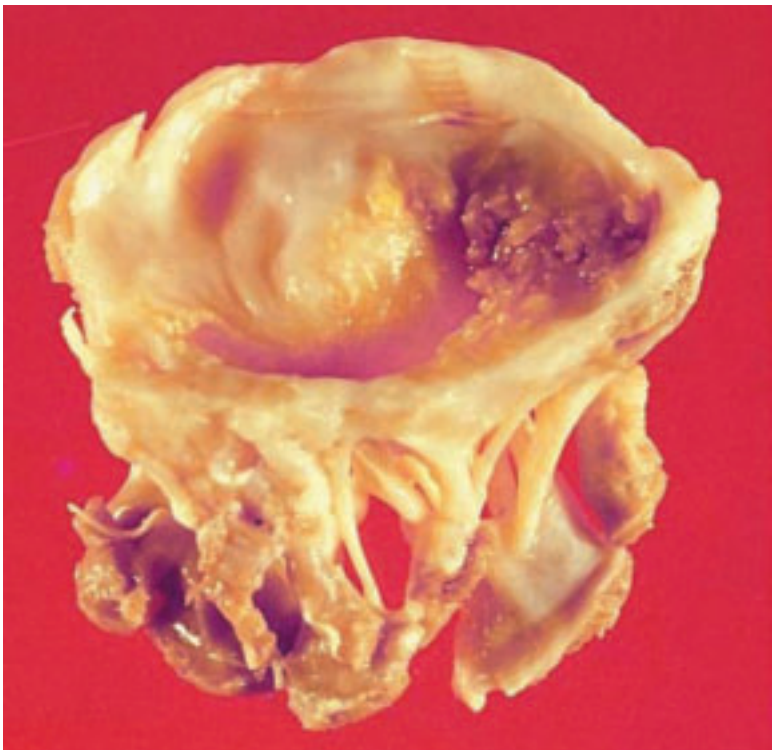

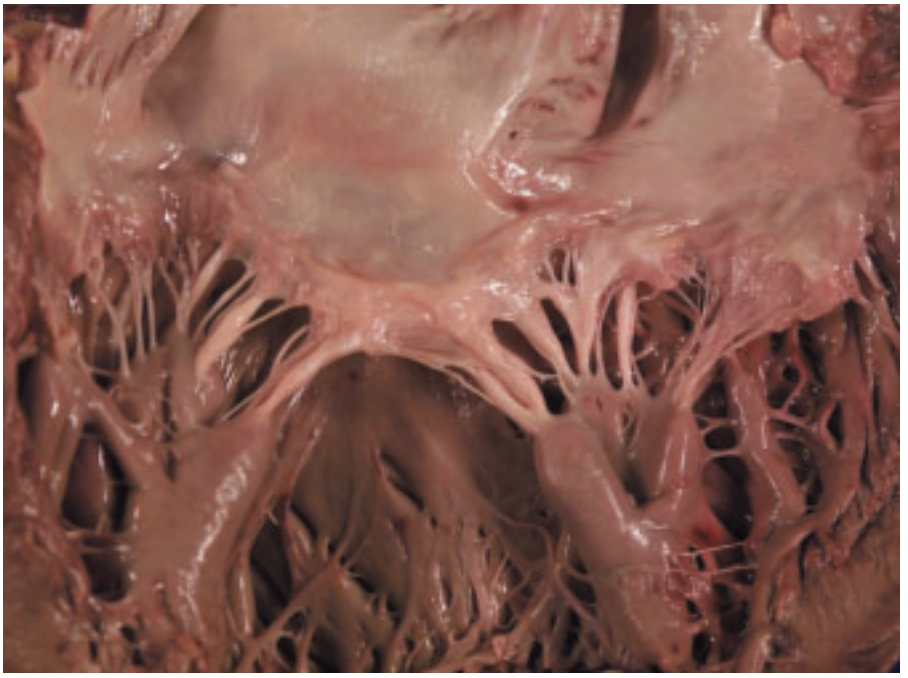

1-40. Several mitral valve chordae are thickened in this patient with micronodular cirrhosis. This association has been noted more often in patients with alcoholic cirrhosis, and the pathogenesis is believed to be related to failure to detoxify an unknown substance that elicits an endocardial overlay lesion in some chordae.

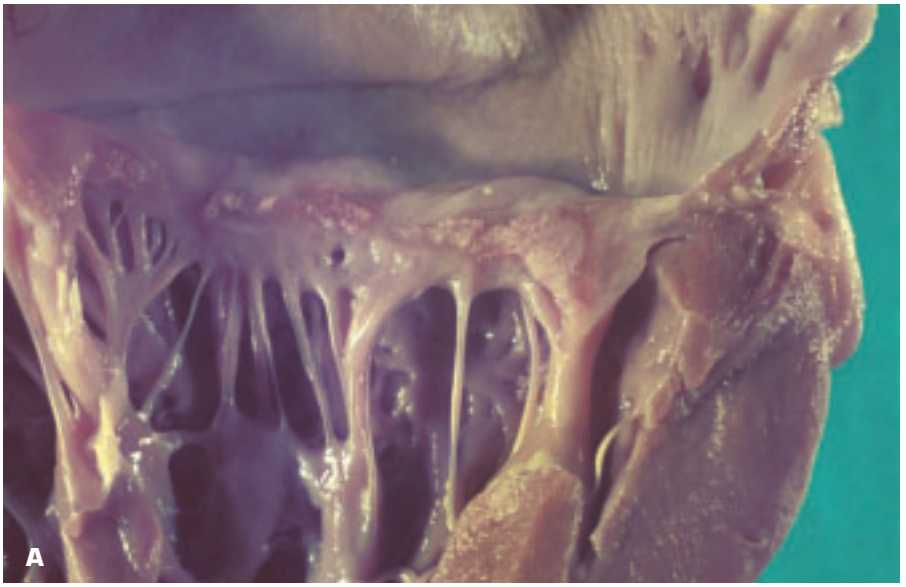

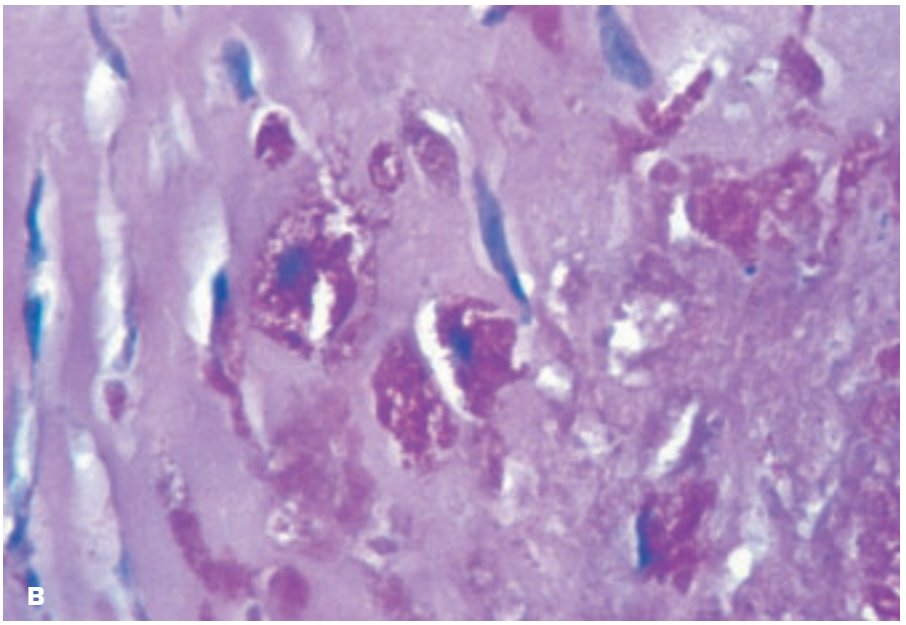

1-41. A. Mitral stenosis in Whipple disease: healing vegetations lie along the contact area of the cusps, which show fibrosis and chordal fusion. **B.** Histology shows histiocytes containing abundant periodic acid-Schiff–positive intracellular material with ghost outlines of bacteria in between.

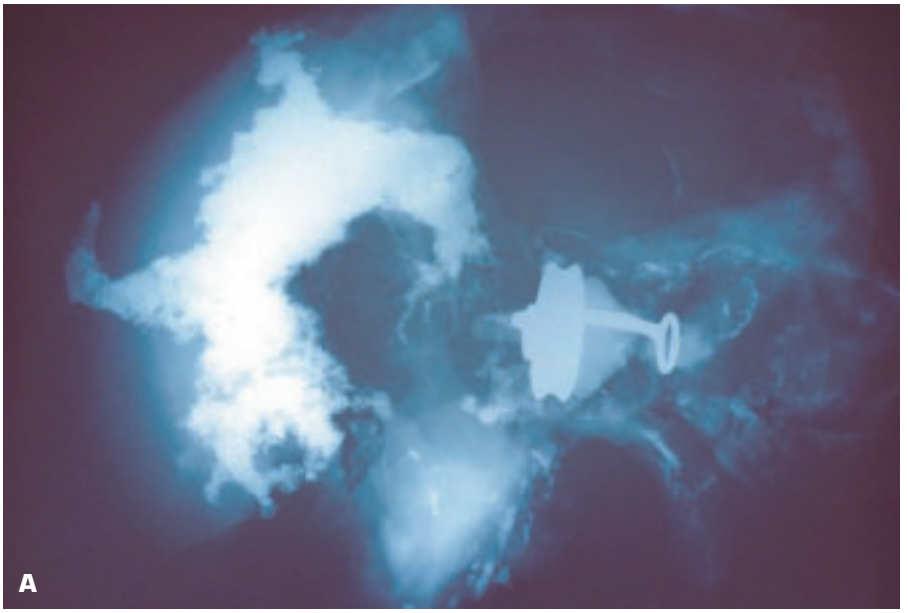

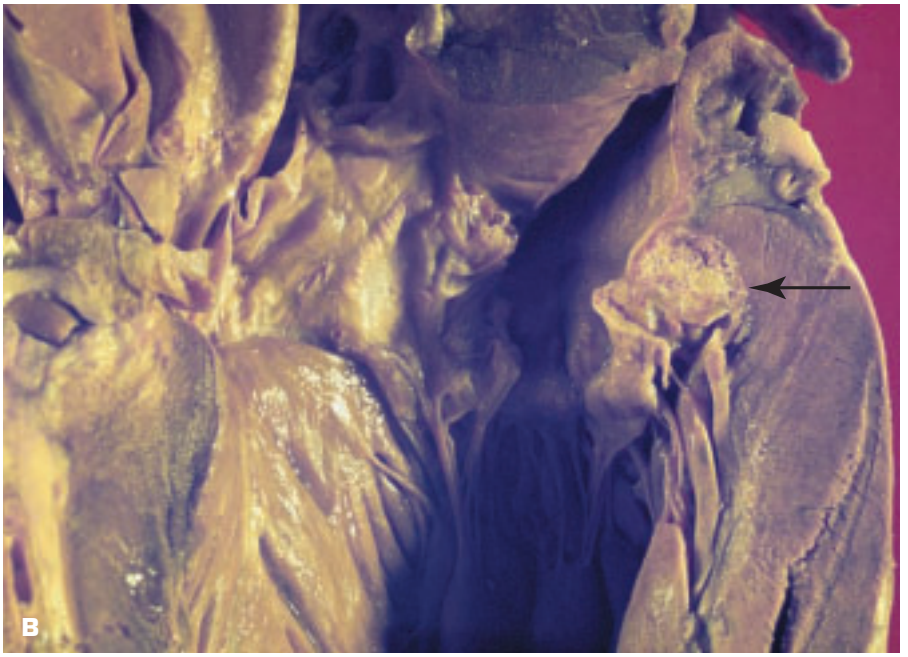

1-42. A. Radiograph of heart with an aortic prosthesis showing massive calcification of the mitral annulus, which is C shaped due to the anterior mitral leaflet making up part of the annulus. **B.** Mitral annular calcification (*arrow*) lies behind the mitral cusp in this sectioned heart. In patients who receive hemodialysis, the calcified material may become liquified and may mimic an abscess in appearance.

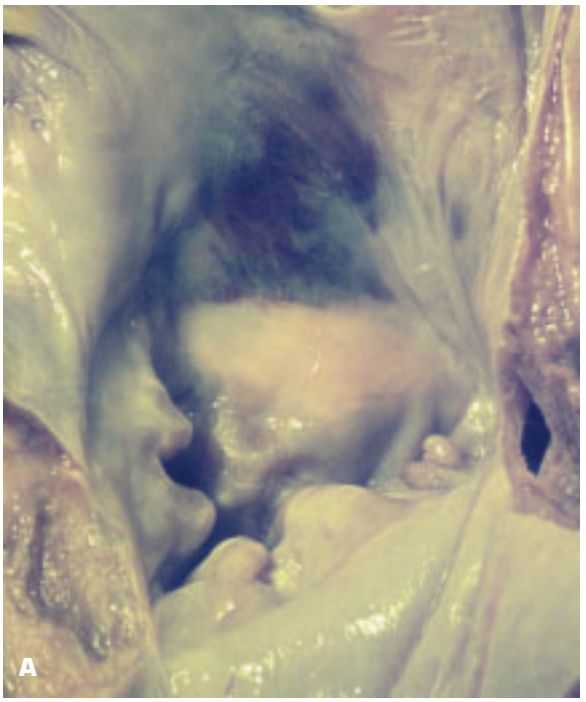

1-43. Floppy mitral valve. **A.** Left atrial view of intact mitral valve showing hemorrhoidal appearance due to multiple hooding of the valve. **B.** Opened mitral valve showing multiple redundant folds (hoods) on posterior leaflet prolapsing back into the left atrium. Intervening portions of the cusp appear normal. **C.** Hoods develop at sites of absent fibrosal collagen and expanded spongiosa (loose connective tissue rich in acid mucopolysaccharide). *(continued on next page)*

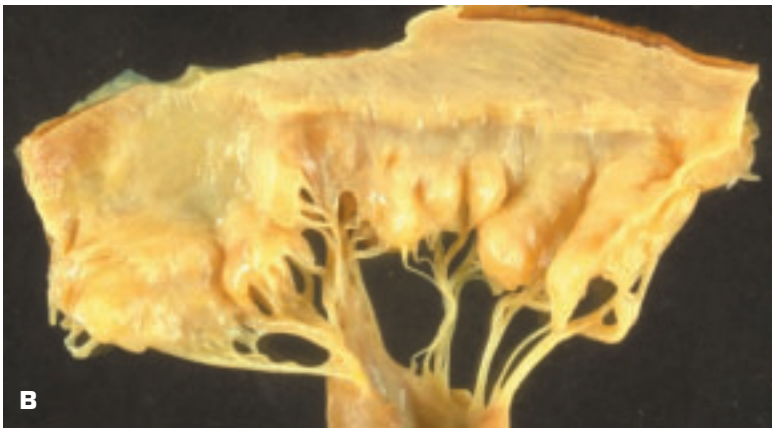

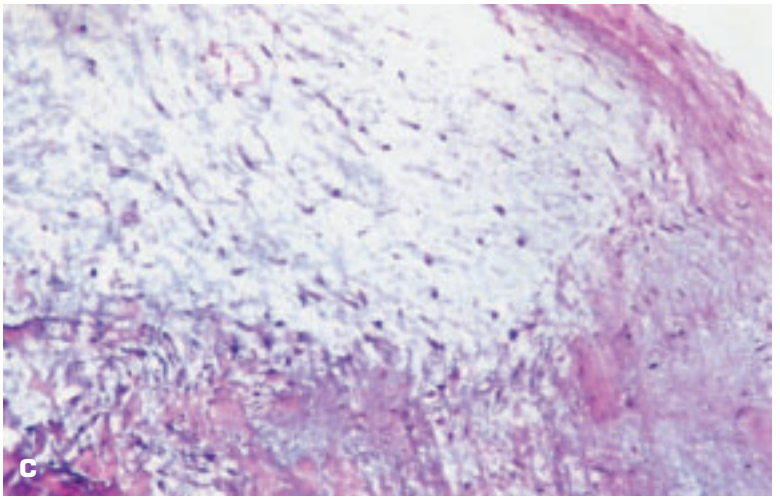

1-43. *(Continued)* **D.** Endocardial friction lesion of endocardium behind chordae. **E.** Histologic appearance of the friction lesion showing red staining collagen layer expanding the endocardium. Chordal rupture may result in some cases.

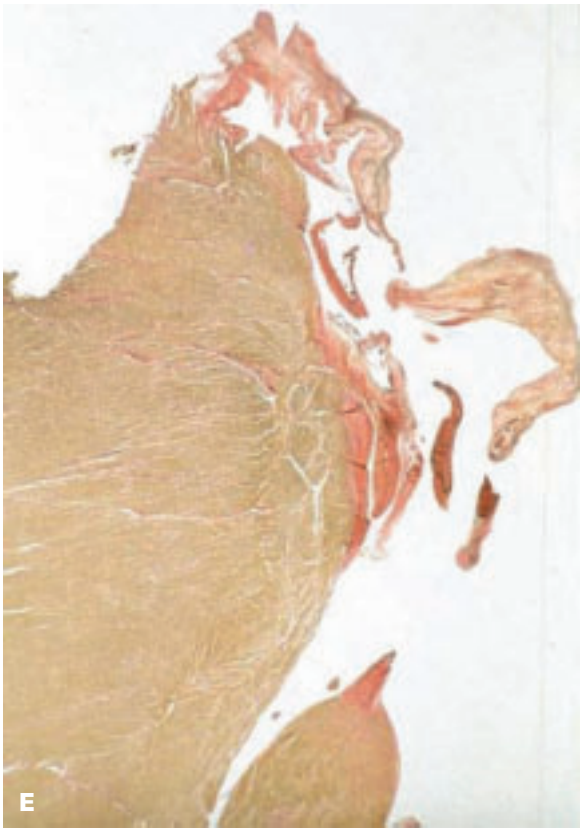

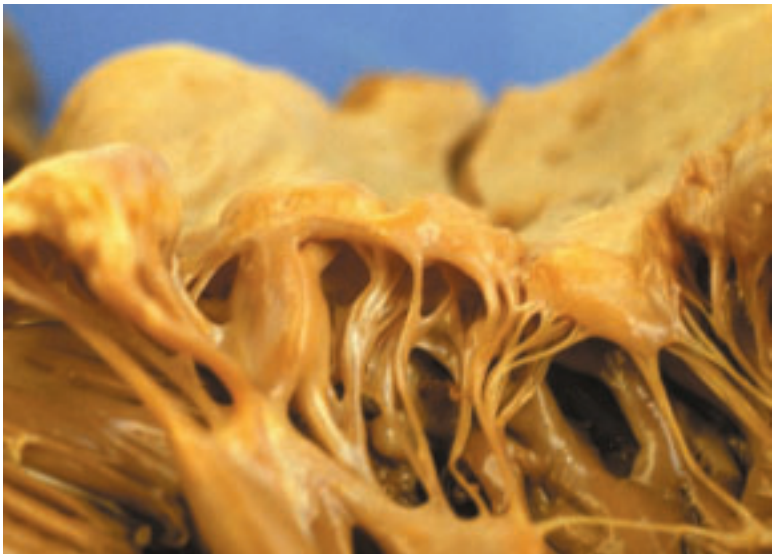

1-44. Floppy mitral valve of long duration shows diffuse cuspal fibrosis and chordal thickening that may mimic healed rheumatic fever.

1-45. Infective endocarditis complicating a floppy mitral valve.

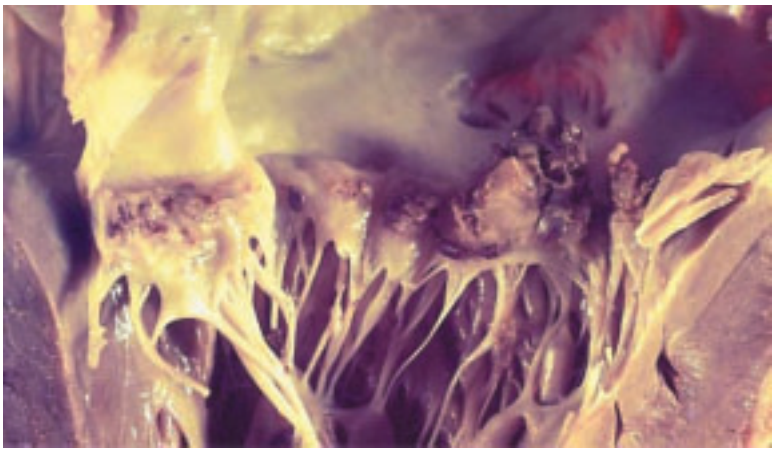

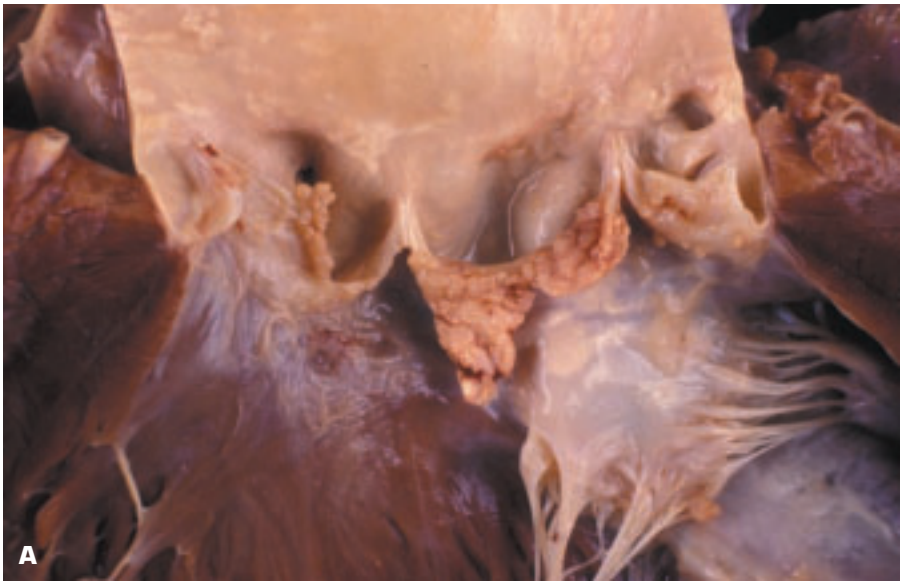

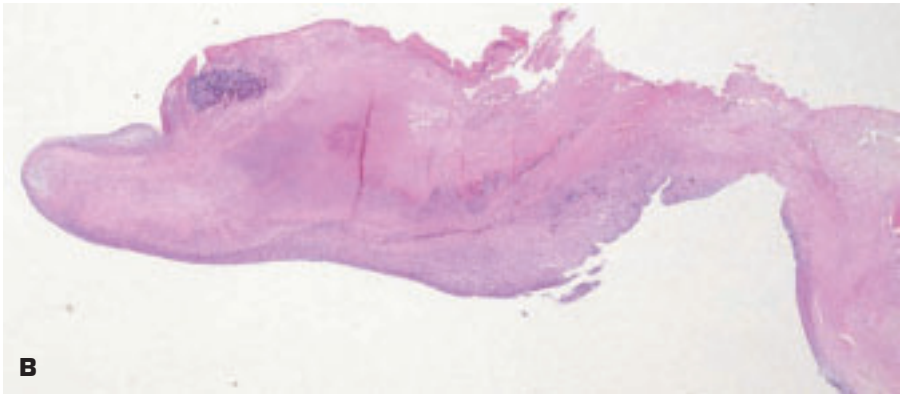

1-46. A. Infective endocarditis of a normal aortic valve with perforation of two valve cusps. **B.** Histologic appearance of aortic valve infective endocarditis with focal basophilia due to presence of pus cells within vegetation on the cusp.

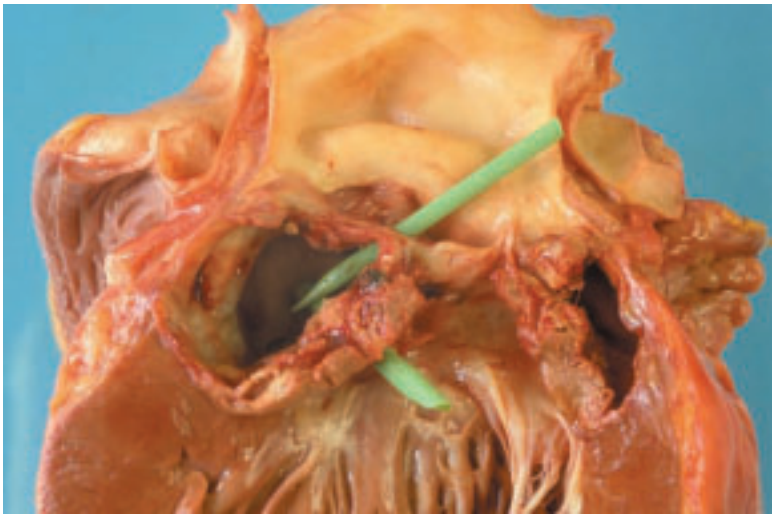

1-47. Massive ring abscess of aortic valve in a patient with Q fever endocarditis due to *Coxiella burnetii* infection. Surgical correction, including aortic root replacement, would be the only way to cure this patient. Alternatively, a valved tube graft from the cardiac apex to the aorta, combined with occlusion of the aortic root, may have been attempted.

1-48. Severe destruction of chordae and anterior cusp of mitral valve due to infective endocarditis caused by a virulent *Staphylococcus aureus* organism.

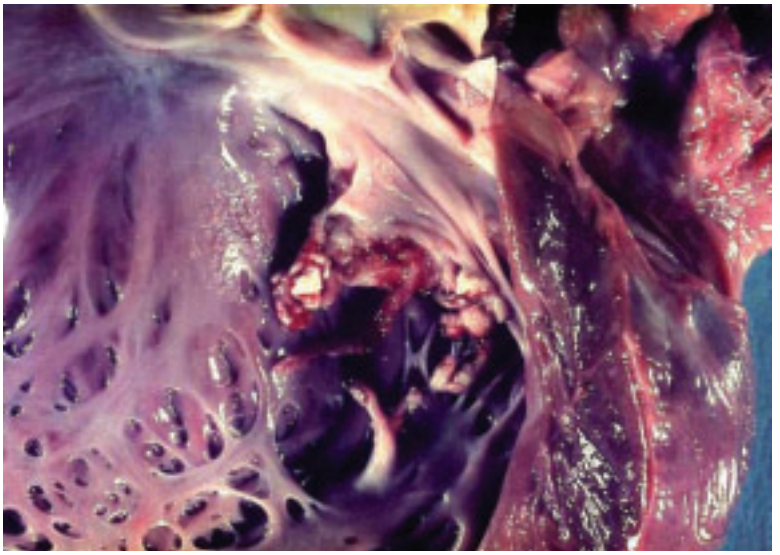

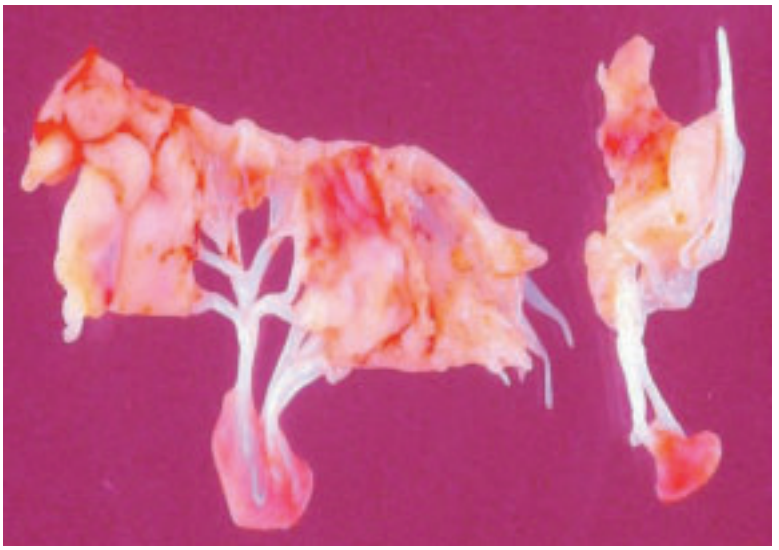

1-49. Surgically excised tricuspid valve for infective endocarditis.

1-50. Because of the low right-sided blood pressure and gentler circulation, vegetations on the right-sided heart valves may attain a much larger size than on the left side of the heart. These two vegetations filled much of the right ventricle and the right atrium.

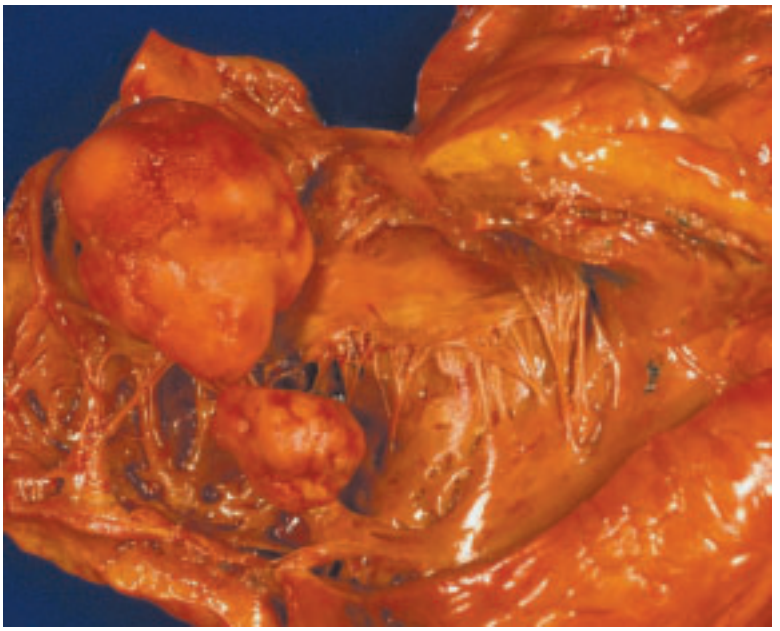

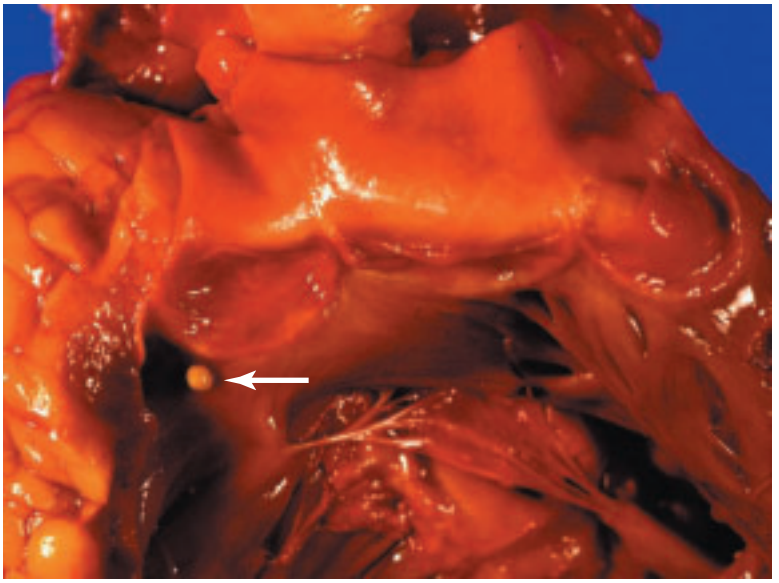

1-51. Endocardial vegetation (*arrow*) close to pulmonary valve due to infection by *Candida albicans.*

1-52. Ruptured mycotic aneurysm of anterior leaflet of mitral valve due to infective endocarditis. Note that the aneurysm faces into the lower-pressured left atrium.

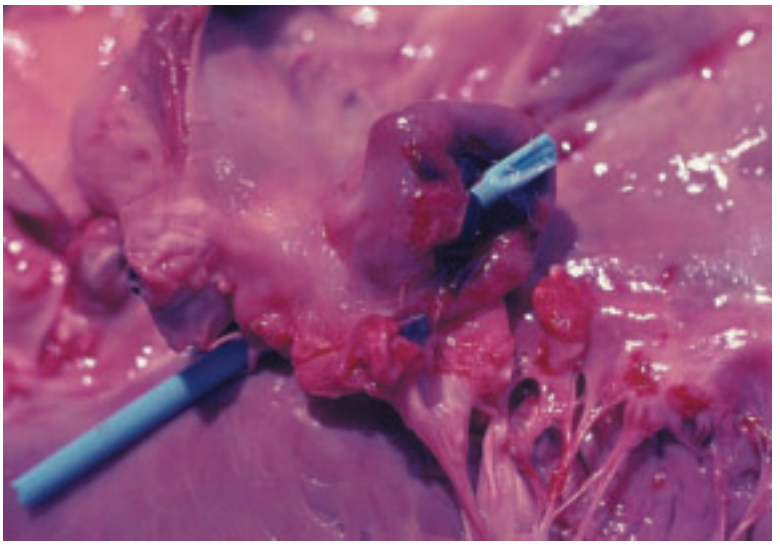

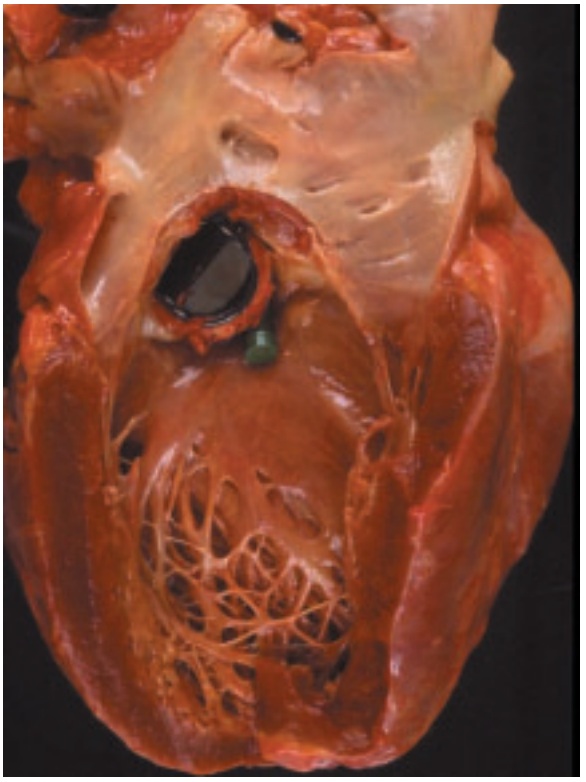

1-53. Prosthetic valve endocarditis occurs in the host tissue adjacent to the prosthesis and leads to prosthetic ring sutures pulling out of the infected host tissue, causing incompetence of the valve. Plastic probe indicates this area in the photograph.

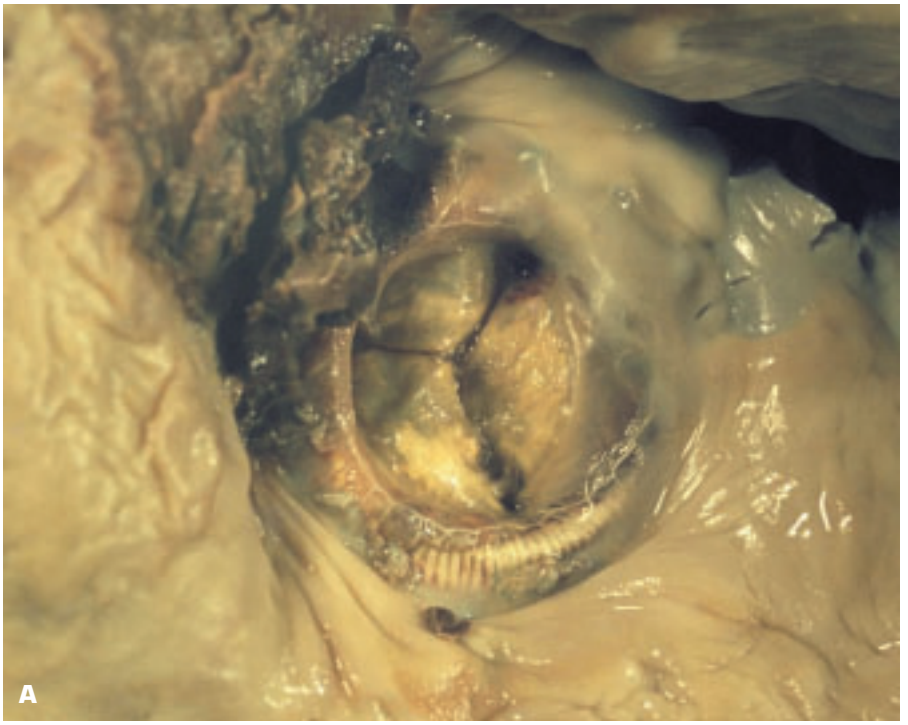

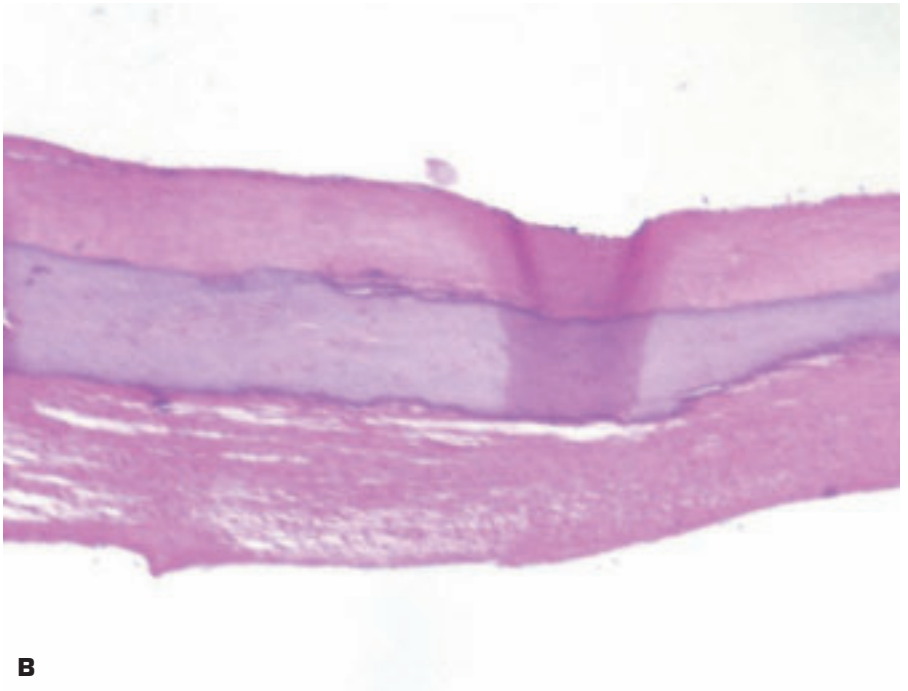

1-54. A. Calcification of a Hancock porcine aortic valve prosthesis has produced severe mitral stenosis in this young girl. Thrombus overlying the atriotomy wound site attests to the short duration that the prosthesis had been in situ. **B.** Histology of a cusp shows central calcification of the cuspal collagen in an area that would have become fixed last during glutaraldehyde fixation. Unlike formaldehyde, glutaraldehyde is a poorly penetrating fixative.

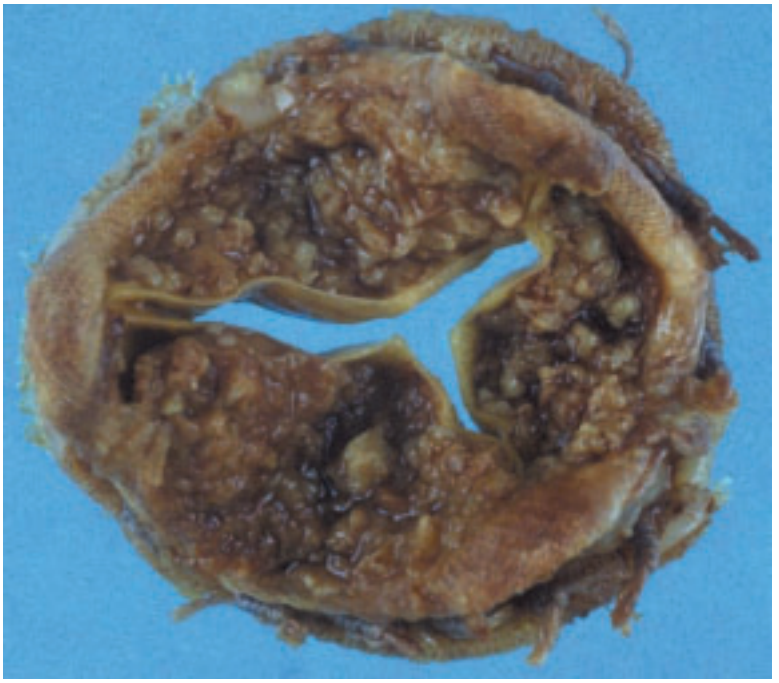

1-55. Massive thrombus fills the valve pockets on the outflow aspect of this porcine aortic valve prosthesis, leading to prosthetic valvular stenosis.

1-56. Surgical suture looped around one strut of this bovine pericardial heart valve prosthesis has tilted up the prosthesis so that it greatly obstructs the subaortic outflow tract of the left ventricle and led to death of the patient soon after surgery. The prosthesis was inserted from the left atrial aspect, and the strut and suture were invisible to the surgeon performing the operation.

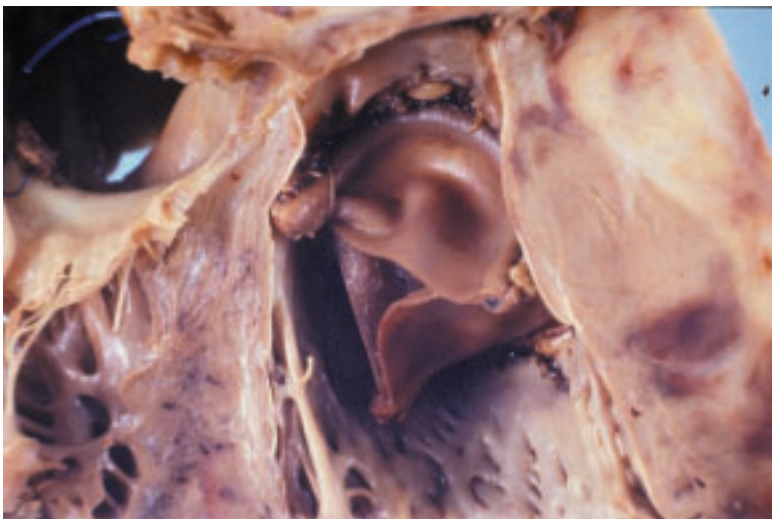

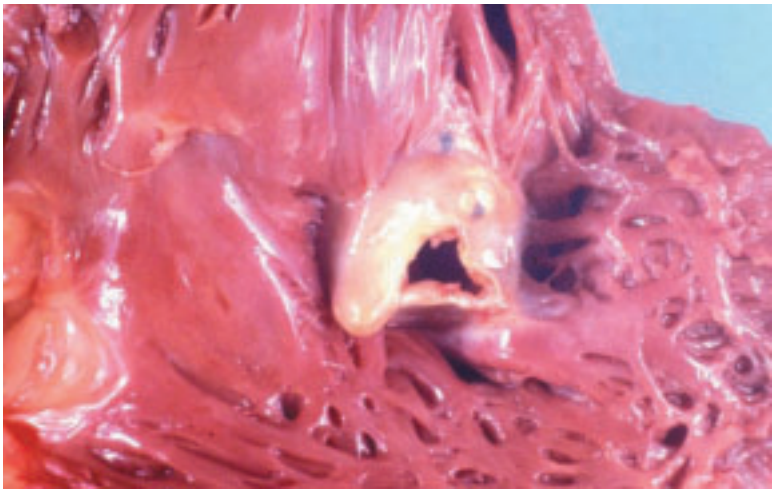

1-57. Pannus tissue overgrowth has produced stenosis of this Ionescu-Shiley bovine pericardial mitral valve prosthesis and obscured the original cusps. Some bland fibrin-platelet thrombus is present on the free margins of the cusps.

1-58. Severe prosthetic stenosis of this St. Jude Medical mechanical prosthesis has resulted from bilateral thrombus at the hinge mechanism area that has led both cusps to be fixed in the slightly open position.

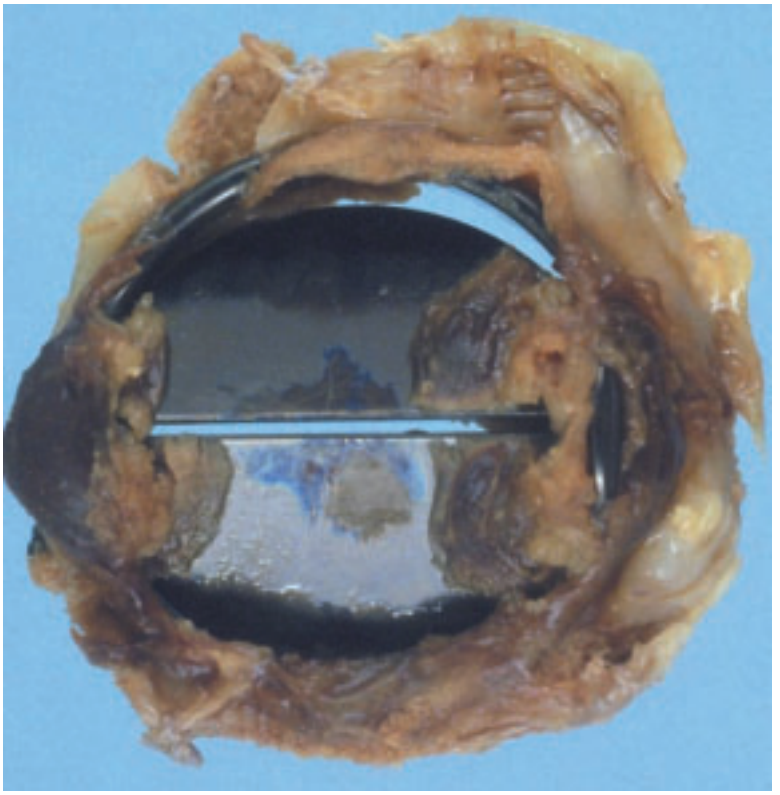

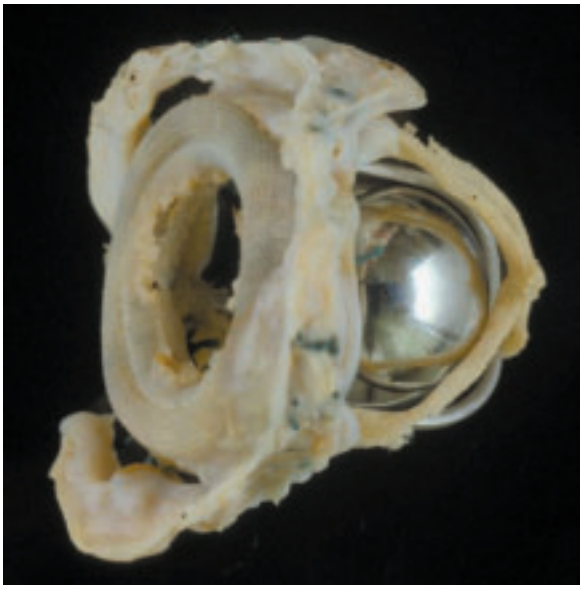

1-59. Cloth wear in this Starr-Edwards ball valve mitral prosthesis has led to partial detachment of the cloth from the cage struts. Abundant thrombus had become attached to the free cloth, and the cloth wear became apparent only after the thrombus had been cleared from the cloth surface.

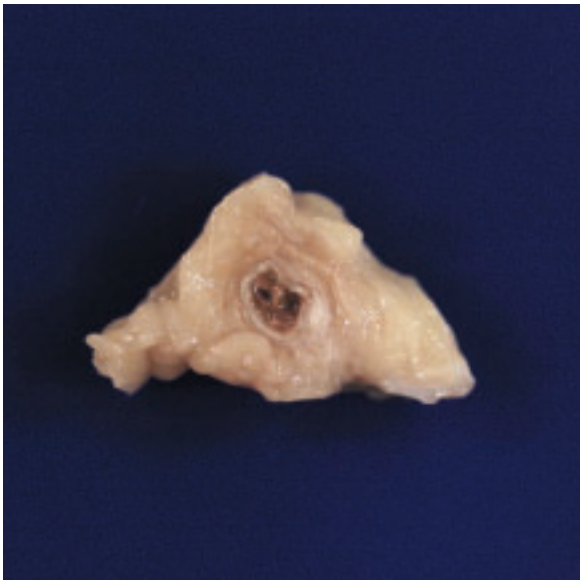

1-60. Totally occlusive thrombus fills the lumen of this atherosclerotic coronary artery.

1-61. Top panel shows a recent regional, anteroseptal, transmural myocardial infarct (*left*) as a pale area in the left ventricle. Propagated red thrombus is seen within sections of the left anterior coronary artery (*right*). Bottom panel (*left*) shows a ventricular slice with a healed posterior myocardial infarct, plus a more recent, reperfused infarct that appears hemorrhagic in appearance. The thrombosed causative coronary occlusion is seen in sections of the coronary artery (*right*).

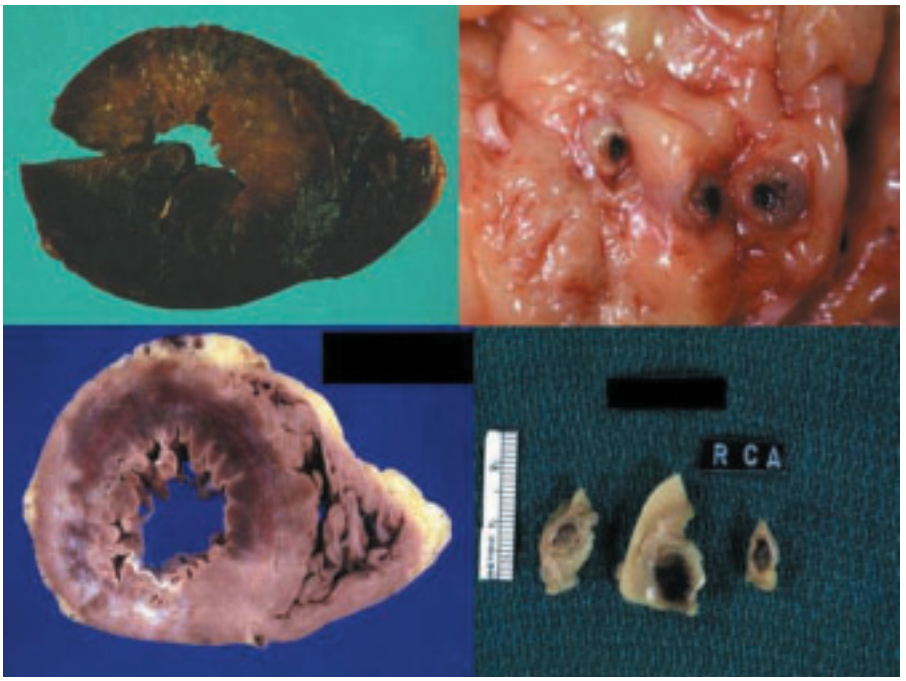

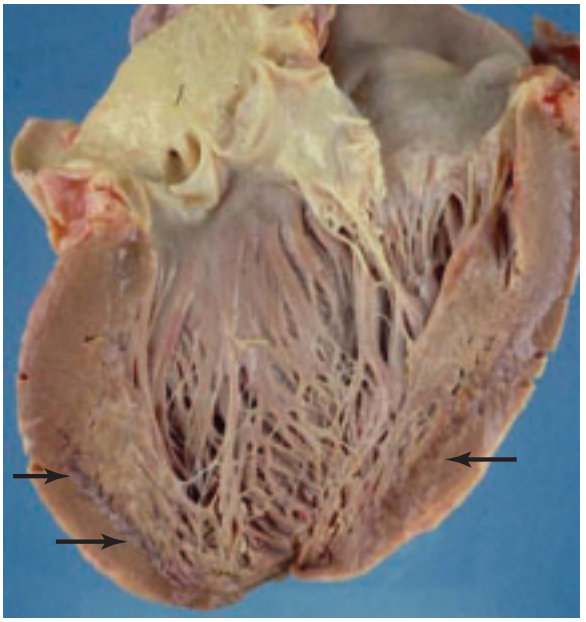

1-62. Global, subendocardial infarction (arrows) of the left ventricle has resulted from more than 80% stenosis of all three major epicardial coronary arteries. The subendocardial myocytes are replaced by fibrous tissue, and ongoing acute ischemic necrosis of small groups of myocytes was noted histologically.

1-63. Thrombus (*arrow*) lies within longitudinally opened atheromatous coronary artery (*top*), and segments (*middle*) of transversely sectioned coronary artery contain occlusive thrombus. Bottom picture shows close-up view of ruptured fibrous cap of an atheromatous plaque with thrombus (*right*) in direct contact with cholesterol crystals (*left*).

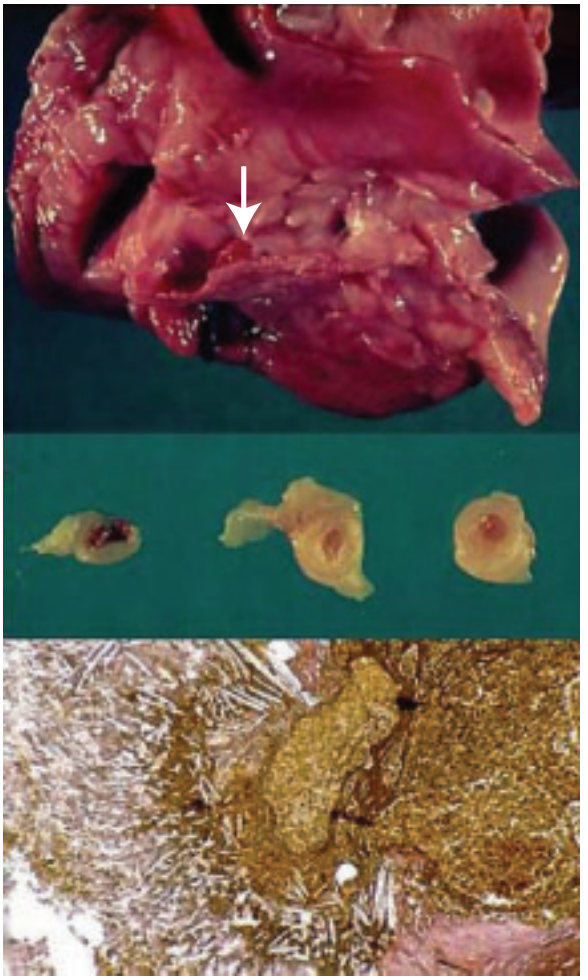

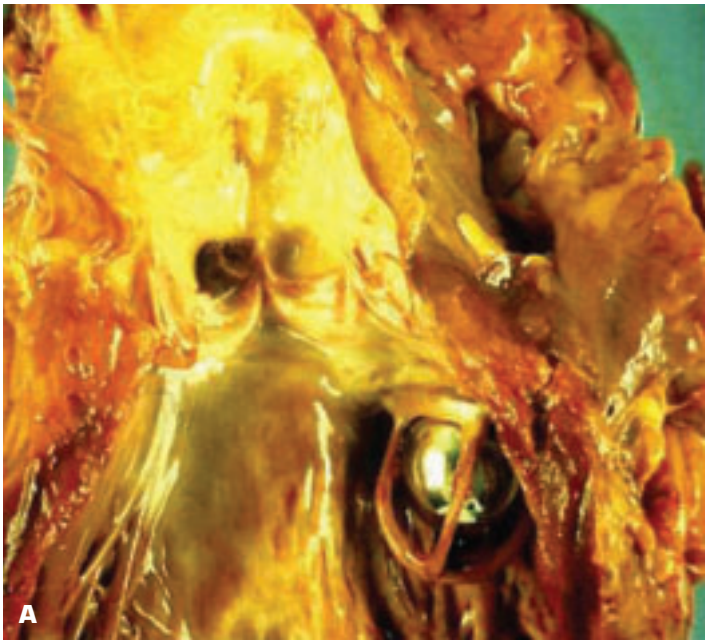

1-64. A. Thromboembolus (derived from left atrial aspect of mitral valve prosthesis) totally occludes ostium of left coronary artery in aortic root. **B.** Histologic appearance of the occluding thrombus.

1-65. Acute dissecting aneurysm (*arrow*) of proximal left anterior descending coronary artery.

1-66. Stent lies within a resected segment of coronary artery.

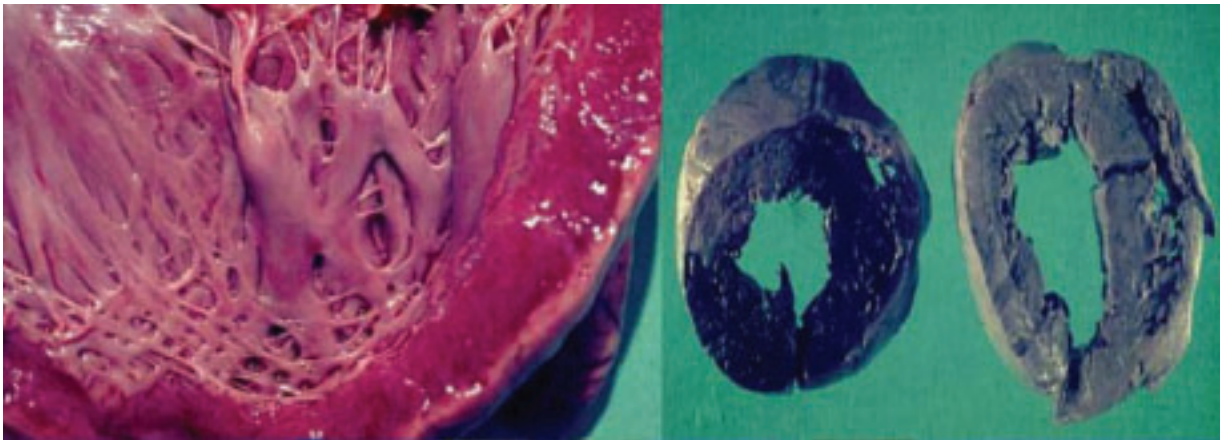

1-67. A very recent (about 4 hours by history) myocardial infarct of left ventricle (*left*) shows only edematous myocardium on its cut surface. Right shows two biventricular slices from the same heart with a 6-hour duration myocardial infarct; the infarct is well delineated as the nonstaining area in the blue-stained left slice that had been incubated with nitroblue tetrazolium.

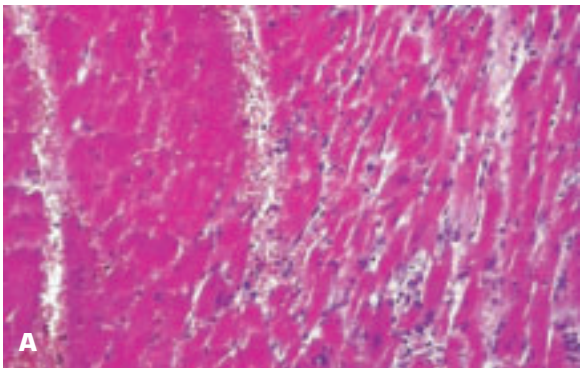

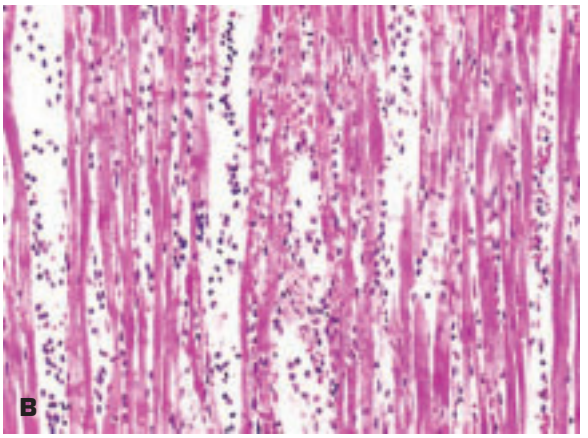

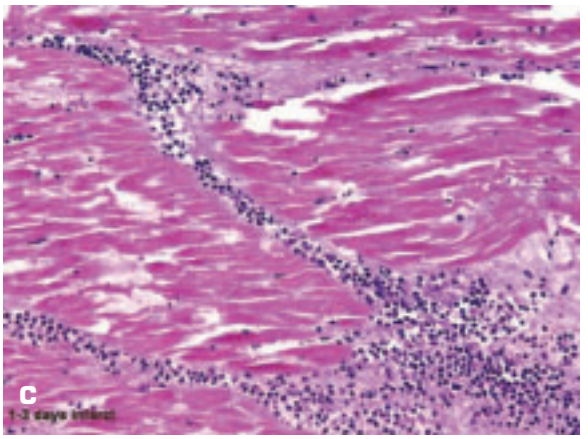

1-68. Histology of acute myocardial infarction. **A.** Edge of an infarct of about 6 hours duration showing coagulative necrosis (*left*) and damaged, viable myocytes (*right*). **B.** Edge of expanding infarct of about 12 hours duration showing contraction band necrosis of myocytes, interstitial edema, plus a prominent polymorphonuclear leukocytic infiltration. **C.** Central portion of a myocardial infarct of about 4 days duration showing neutrophils infiltrating between myocytes showing advanced coagulative necrosis.

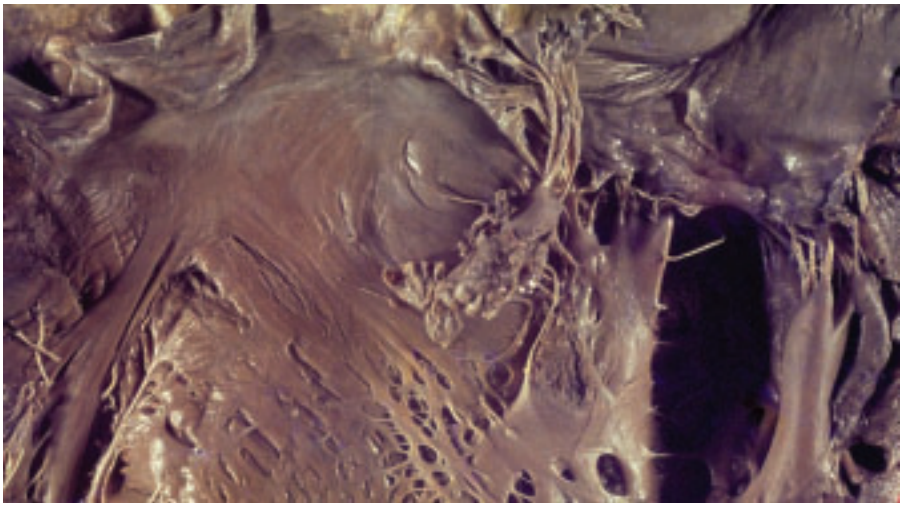

1-69. Ruptured papillary muscle head complicating acute myocardial infarction of left ventricle.

1-70. Acquired ventricular septal defect due to ruptured interventricular septum complicating acute myocardial infarction.

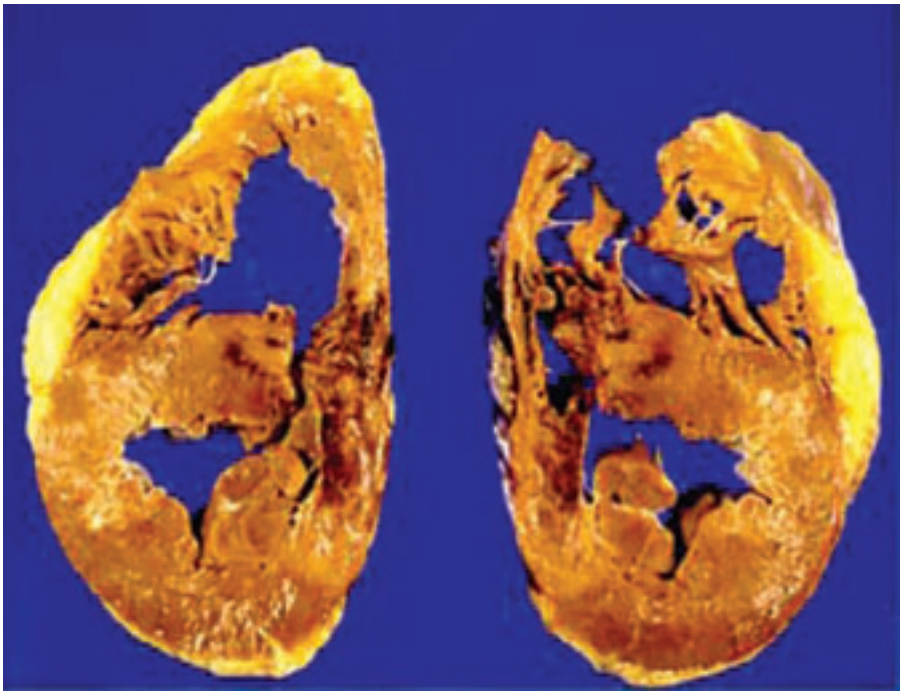

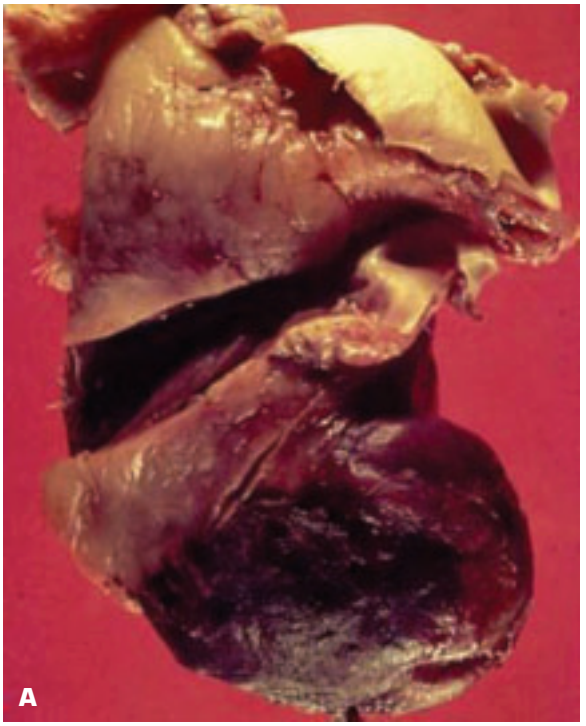

1-71. A. Cardiac aneurysm of left ventricular apex complicating myocardial infarction. **B.** Remnants of the original myocardial wall in the wall of the aneurysm signify the presence of a true cardiac aneurysm.

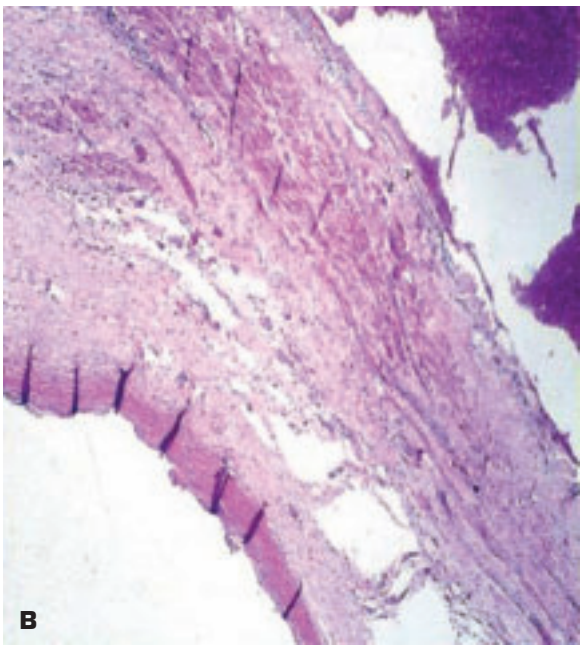

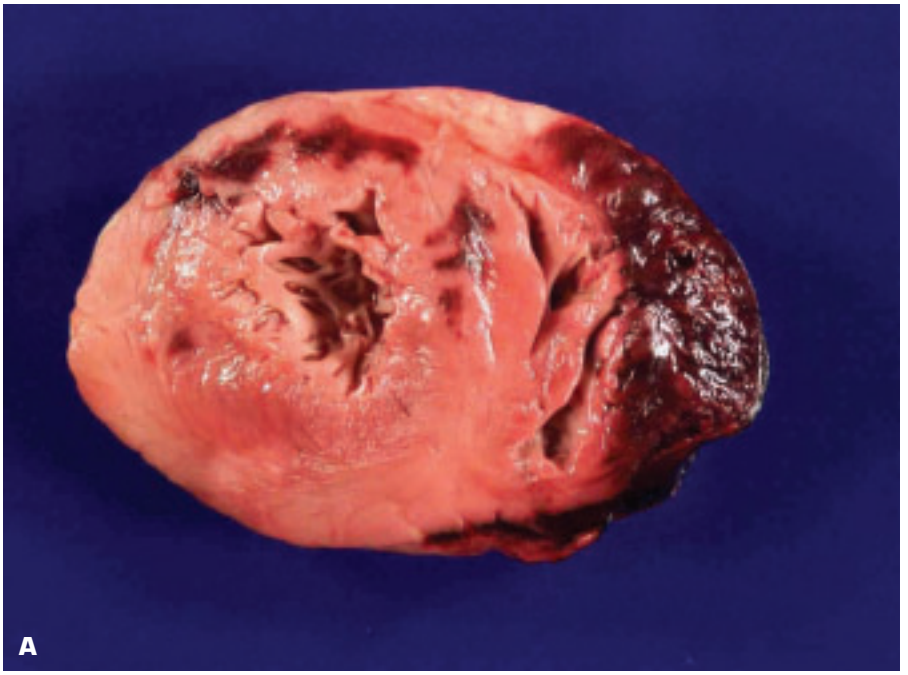

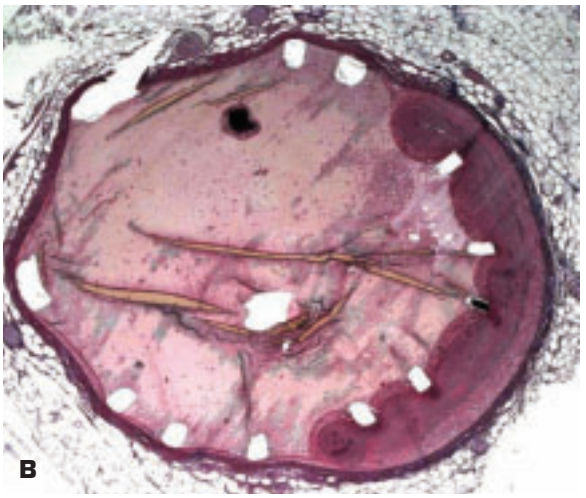

1-72. A. Transverse section of ventricles showing focal hemorrhage within the left ventricle due to a reperfused myocardial infarct. A large intraepicardial hematoma is present over the right ventricle, and death occurred due to massive hemopericardium (cardiac tamponade) that clinically mimicked cardiac rupture. **B.** Section of right coronary artery shows that a stent has been placed within the lumen of a dissection of the artery, and the original lumen is totally compressed. Hemopericardium resulted from intraepicardial bleeding from the dissection, and in turn, this ruptured into the pericardial sac. Bleeding was also favored by the potent antiplatelet agents given for the stent.

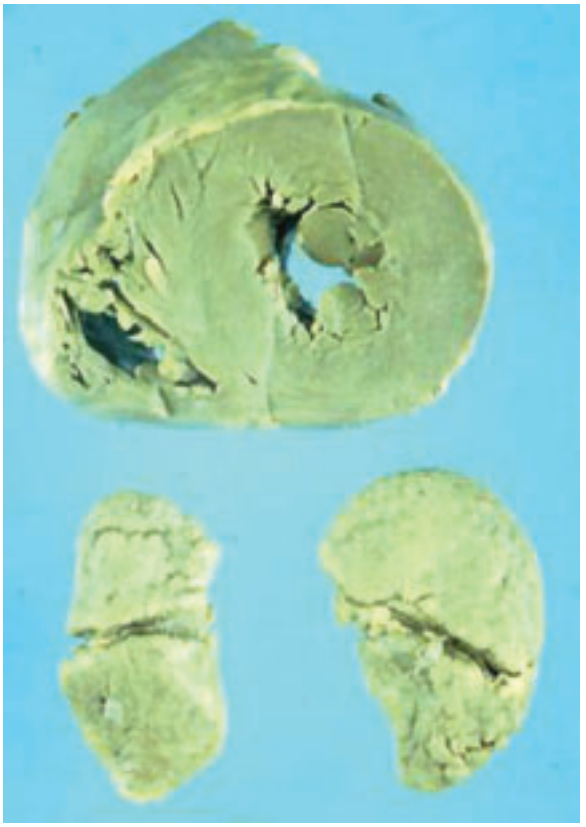

1-73. Transverse biventricular slice of heart showing concentric hypertrophy of left ventricle, incipient chamber dilatation, and the end-stage kidneys from this same patient who had renovascular hypertension.

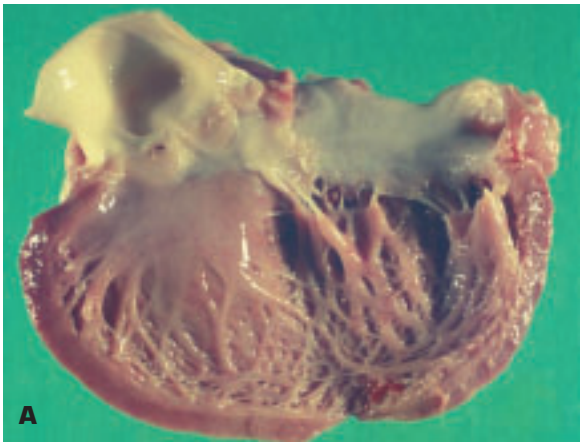

1-74. Acute viral myocarditis. **A.** Dilated, nonhypertrophied heart with slightly mottled myocardium. **B.** Severe interstitial lymphocytic infiltration of the ventricular myocardium with focal loss of myocytes.

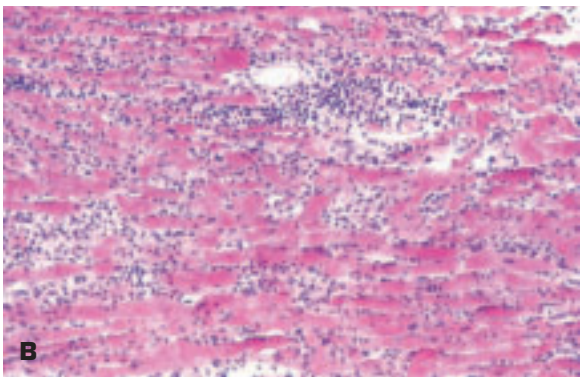

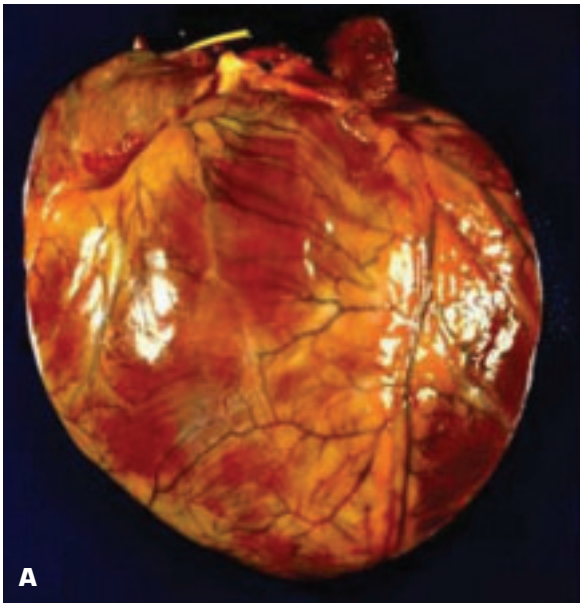

1-75. Idiopathic dilated cardiomyopathy. **A.** Enlarged, football-shaped, globular heart due to generalized chamber hypertrophy and dilatation. **B.** Transverse slice of heart showing diffuse hypertrophy and dilatation of both ventricles. **C.** Longitudinal section of heart showing abundant stasis thrombi at the apices of both ventricles. *(continued on next page)*

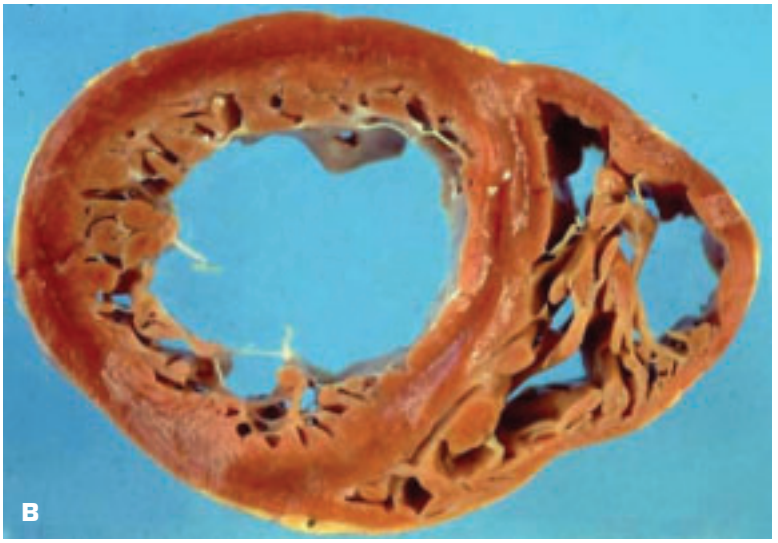

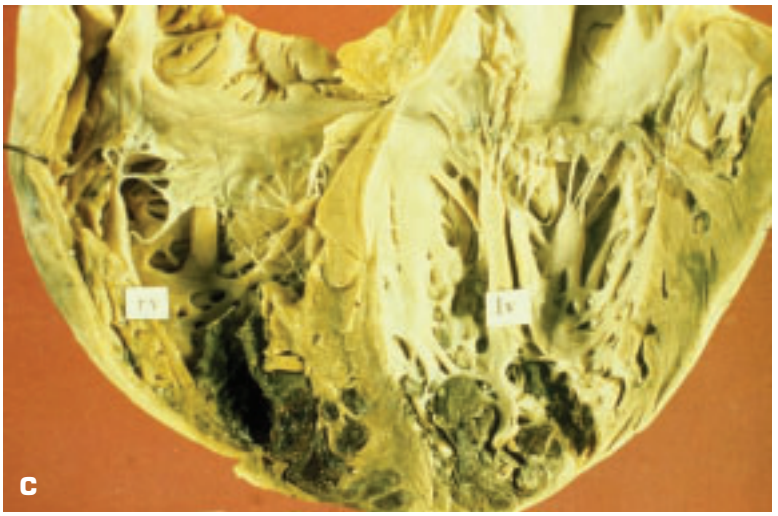

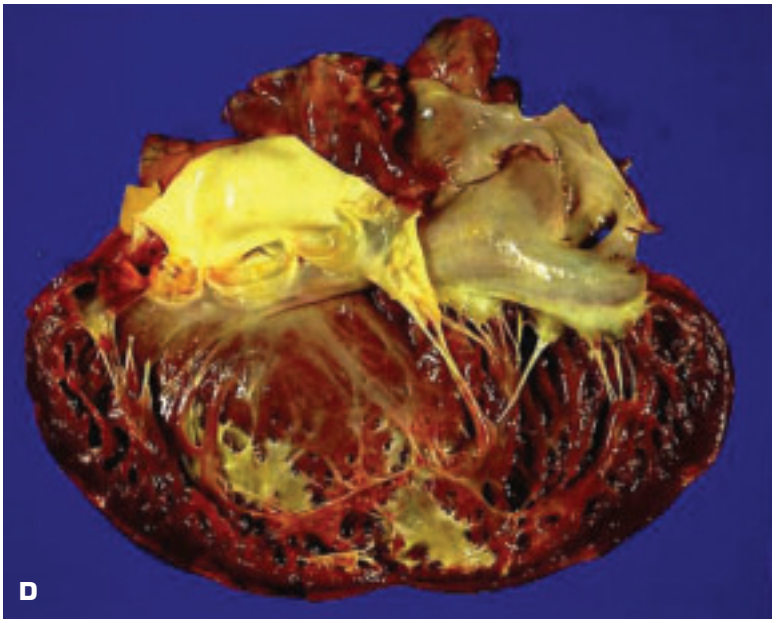

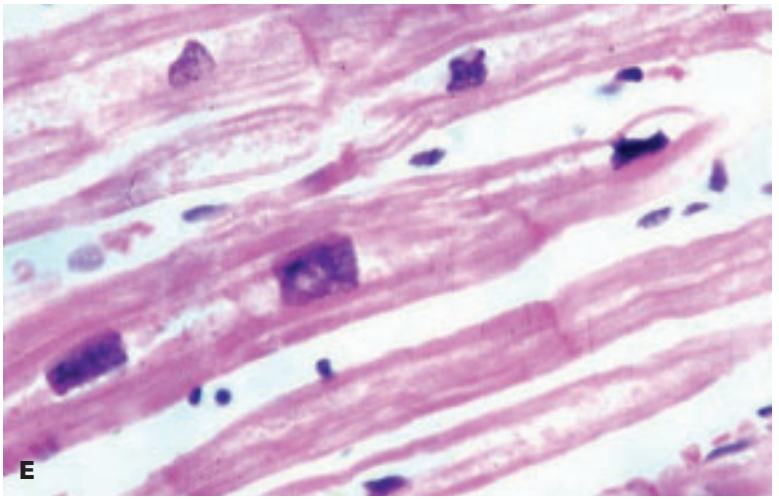

1-75. *(Continued)* **D.** Endocardial scarring near left ventricular apex due to organization of endocardial thrombi. **E.** Histologic evidence of myocyte hypertrophy, namely squared off (box car) nuclei.

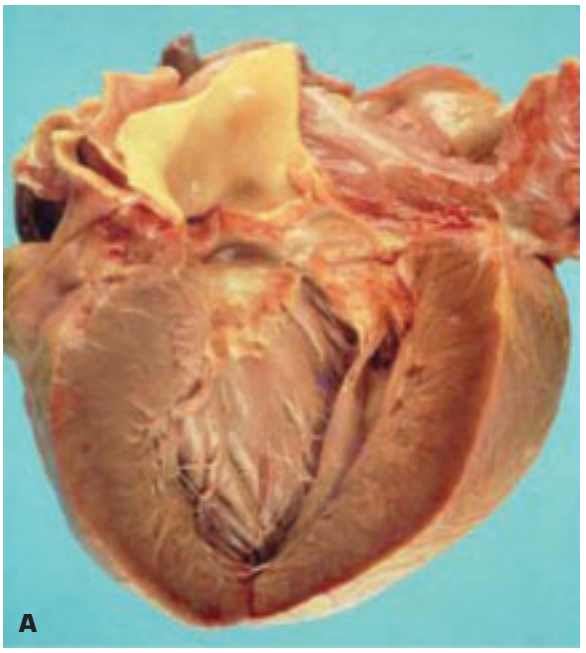

1-76. Hypertrophic cardiomyopathy. **A.** Noteworthy features include massive concentric hypertrophy of left ventricle, inward bulging interventricular septum with mirror image plaque of anterior mitral leaflet, and reactive thickening of anterior leaflet of mitral valve. Note that the mirror image plaque lies more inferiorly than the mitral valve because, during life, tension in its papillary muscles holds the valve at a lower level than after death. **B.** Transverse biventricular slice showing asymmetric septal hypertrophy (interventricular septum is thicker than free wall of left ventricle). **C.** Myocyte disarray in a section taken from midportion of the interventricular septum.

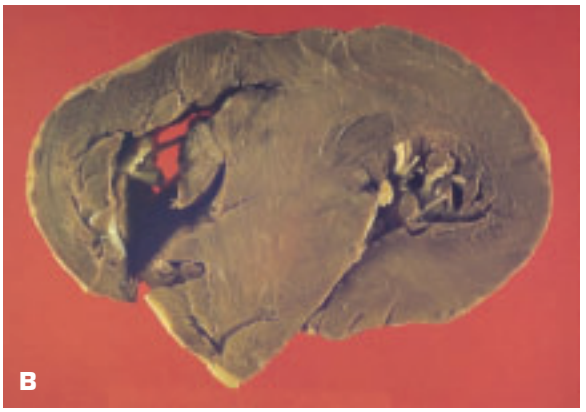

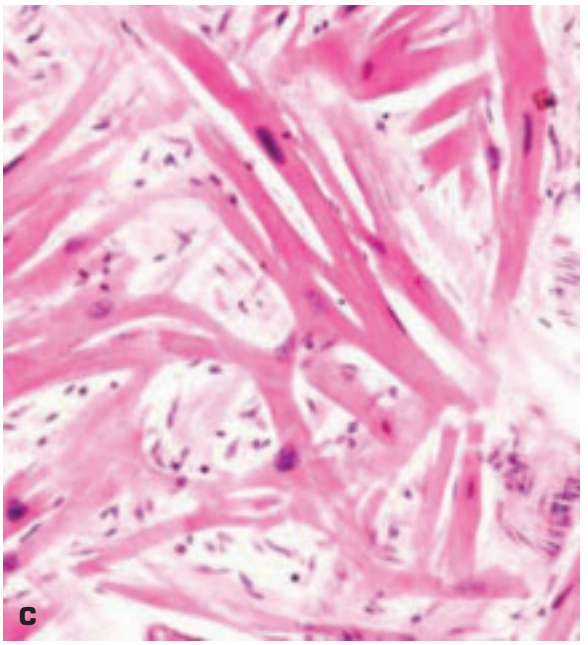

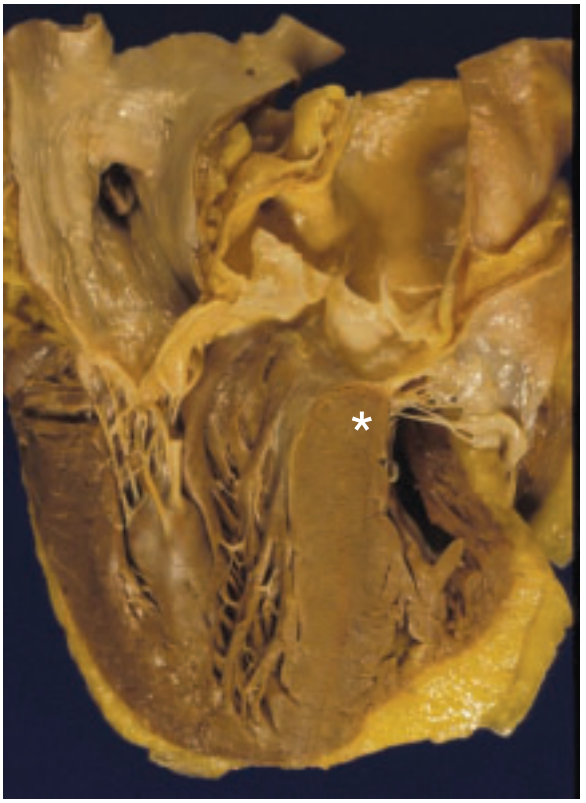

1-77. Sigmoid septum (*) associated with aging. The aorta comes off from the right side of the top of the interventricular septum rather than straight up from its summit. Clinically, a cardiologist may have difficulty distinguishing this entity from true hypertrophic cardiomyopathy.

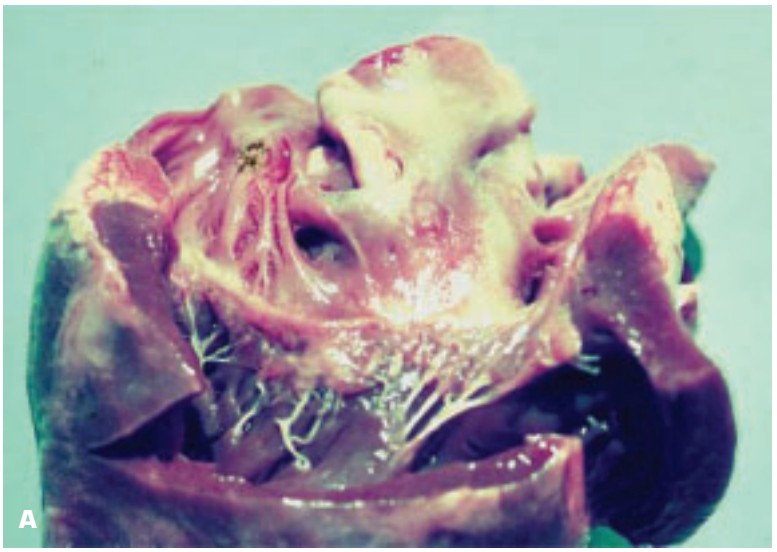

1-78. Restrictive cardiomyopathy. **A.** Amyloidosis of the heart with the amyloid deposits being most visible as granular elevations on the right atrial endocardial surface. **B.** Amyloid nodular deposit in endocardium (Congo Red stain). **C.** Amyloid deposits in a small artery and its surrounding connective tissue (sulphated Alcian blue stain).

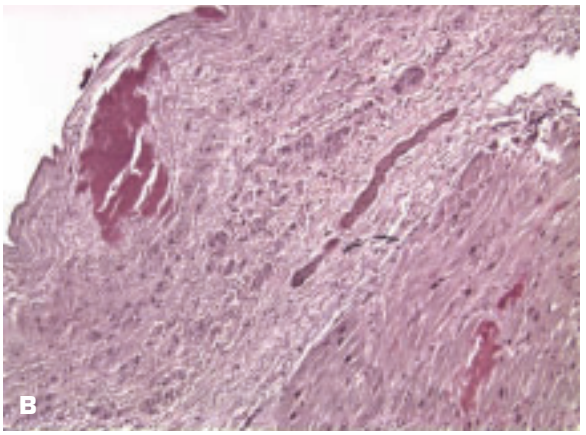

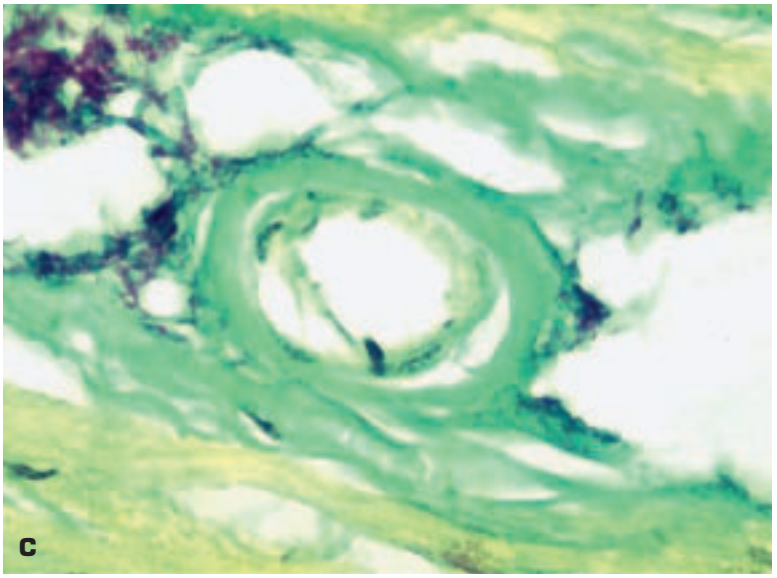

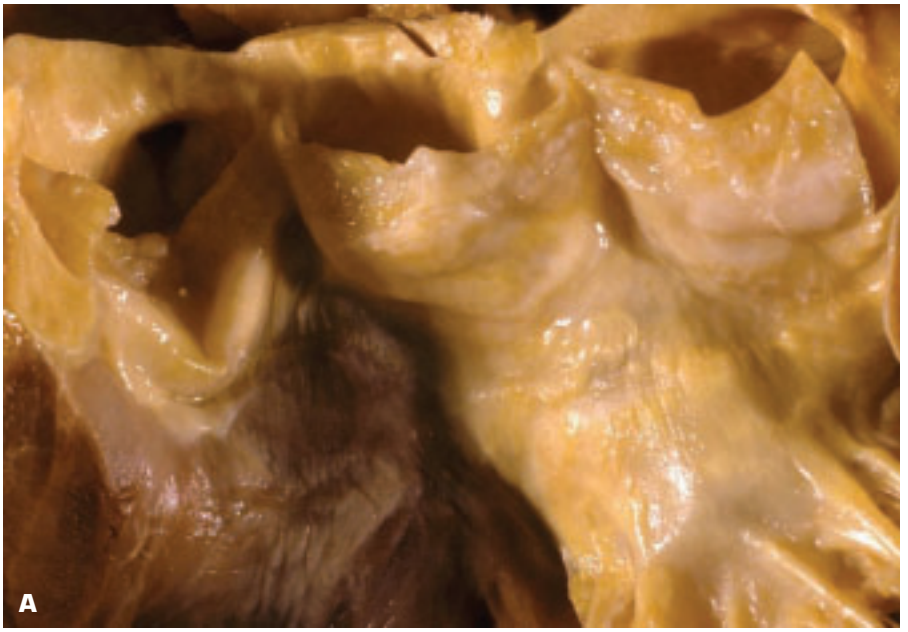

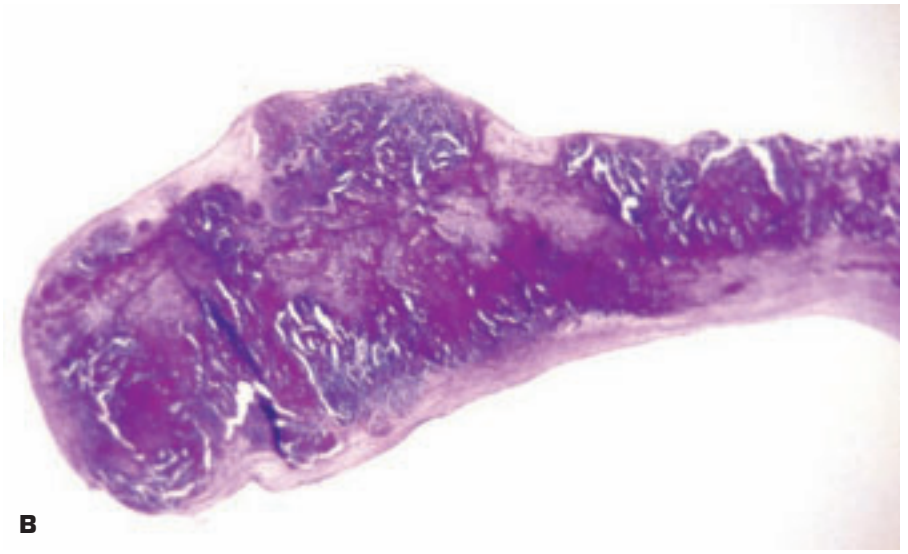

1-79. A. Cardiac amyloidosis with prominent involvement of the left-sided heart valves. **B.** Histology of aortic valve cusp showing massive amyloid deposits (methyl violet stain).

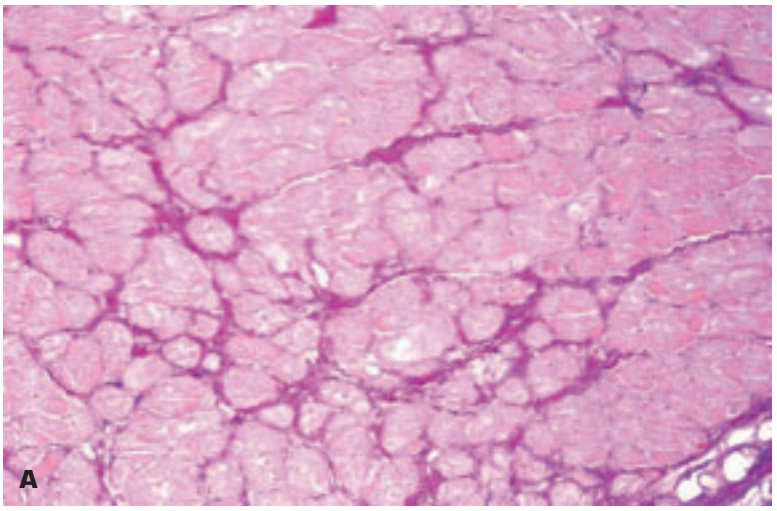

1-80. Other causes of a restrictive cardiomyopathy. **A.** Diffuse interstitial fibrosis of unknown cause led to a restrictive cardiomyopathy in this patient. **B.** Hemochromatosis: the iron-laden heart is a weak heart! Note the greater than normal brown color of the myocardium. **C.** Histology shows massive blue-staining iron deposits within cardiac myocytes (Perl's Prussian blue stain).

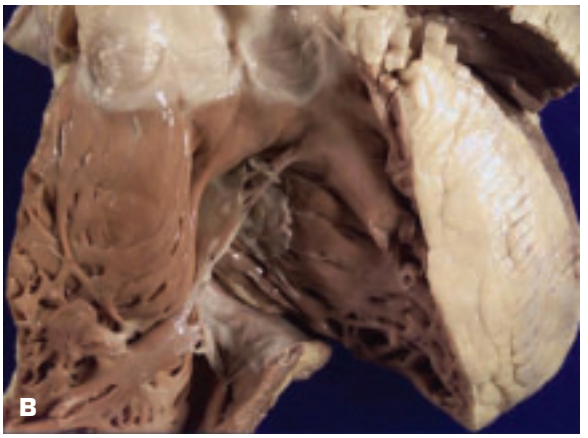

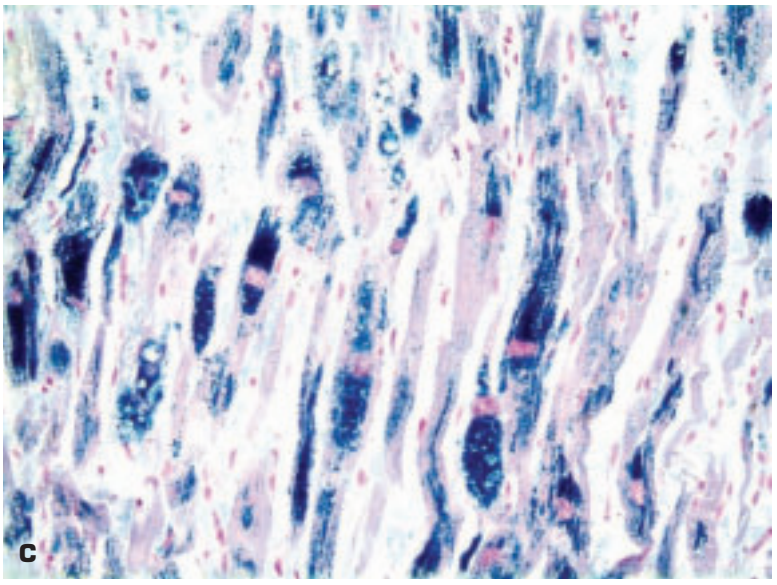

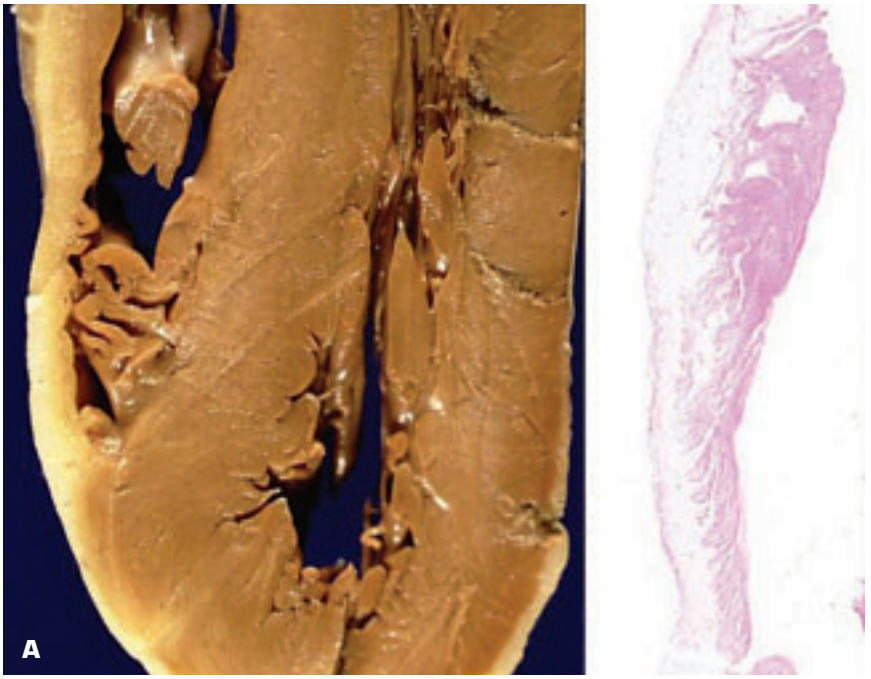

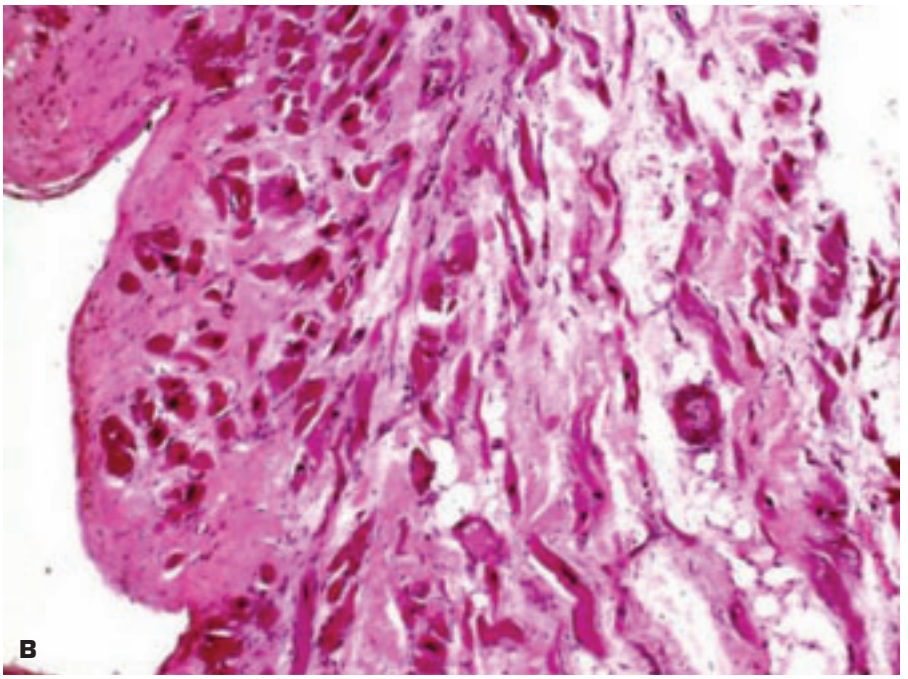

1-81. A. Arrhythmogenic right ventricular dysplasia/cardiomyopathy in a young boy who suffered sudden, unexpected death. Note the greatly thinned apical free wall of the right ventricle (RV). Low-power histology of the RV is shown in the right panel. **B.** Isolated myocytes lie within fibroadipose tissue and fibrous tissue. Some cases may show lymphocytic infiltrates.

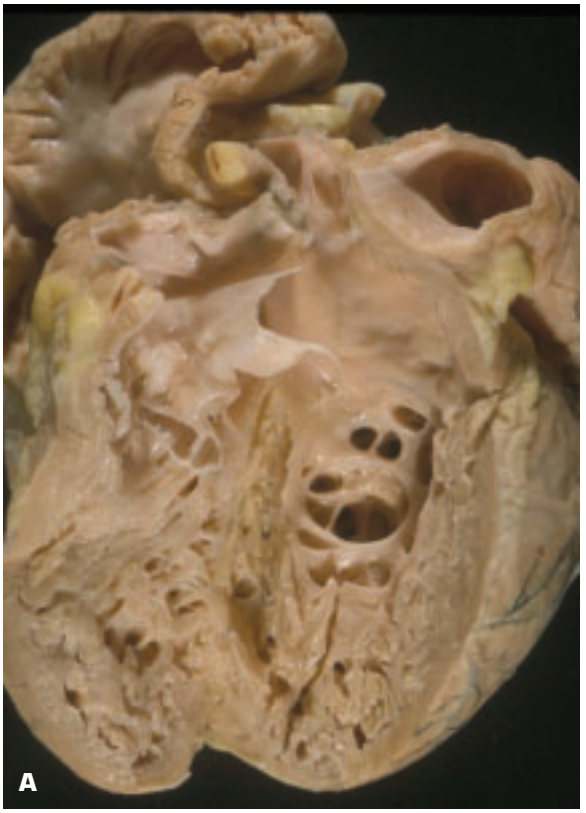

1-82. A. Noncompaction of the left ventricle (NCLV) showing absence of the normal smoothness to the septal wall of the left ventricle; this heart was explanted at the time of cardiac transplantation from a 4-year-old girl with severe heart failure. NCLV will probably be included as a new form of idiopathic cardiomyopathy in future classifications of cardiomyopathy. **B.** Microscopic appearance of noncompacted left ventricle.

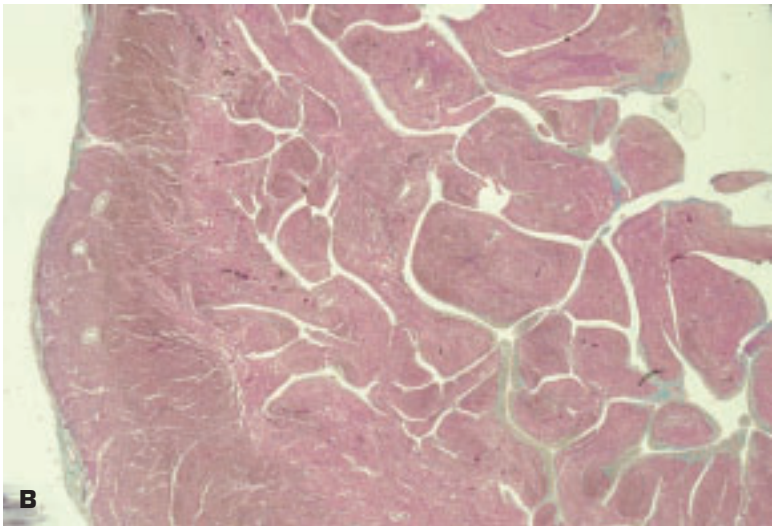

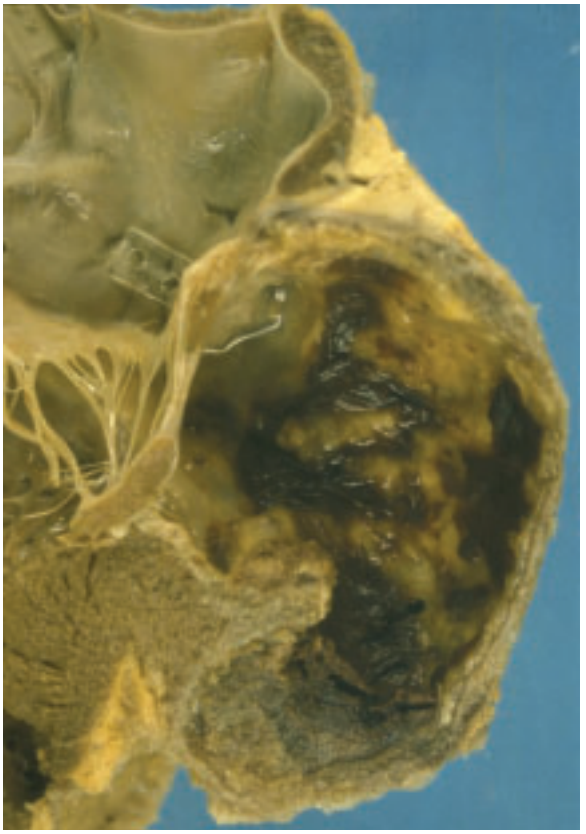

1-83. Idiopathic submitral aneurysm is believed to result from a developmental weakness of the attachment between the mitral annulus and the left ventricle. The condition is more common in certain tribes in southern Africa than in Caucasian populations.

1-84. Orthotopic cardiac transplantation. Note the marked difference in appearance between the normal donor left atrial component and the postrheumatic calcified organized thrombi in the recipient's left atrial component. This donor heart failed due to graft arteriopathy (chronic rejection). Graft arteriopathy is characterized by histologic evidence of myocardial fibrosis and luminal narrowing of both epicardial and intramyocardial coronary arteries (see Fig. 1-86C and D).

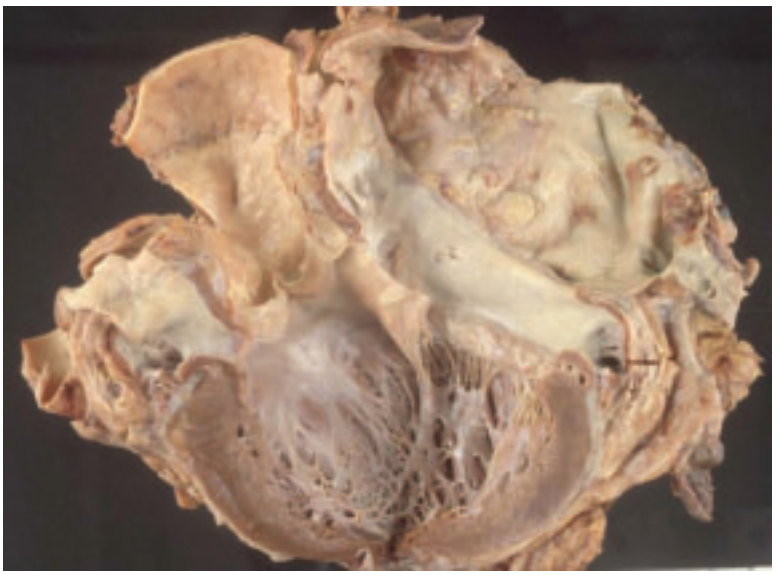

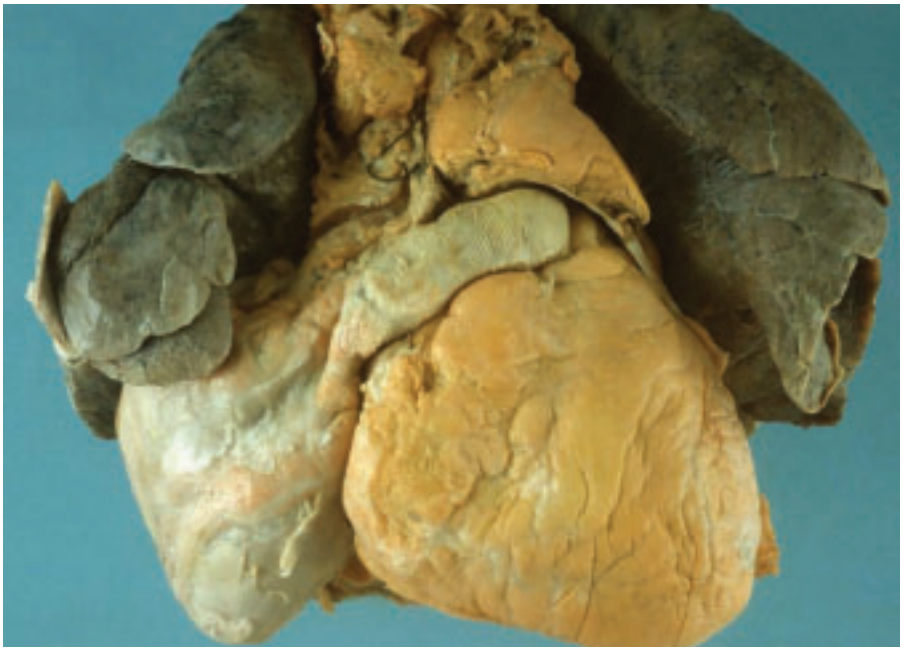

1-85. Heterotopic cardiac transplantation ("piggy-back heart"): the donor heart lies on the left side of the picture, and a Dacron tube graft links the two pulmonary arteries.

1-86. A. Severe acute rejection with arteritis leading to focal areas of ischemic infarction of the left ventricle in an explanted donor heart. Immunosuppression had been discontinued shortly before the heart was removed and replaced by another donor heart. **B.** Histology of severe acute rejection showing marked interstitial lymphocytic infiltration. *(continued on next page)*

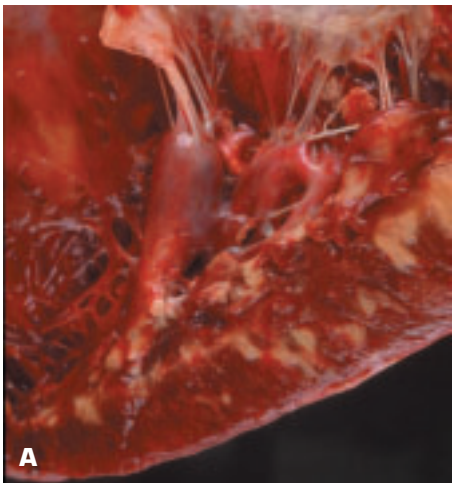

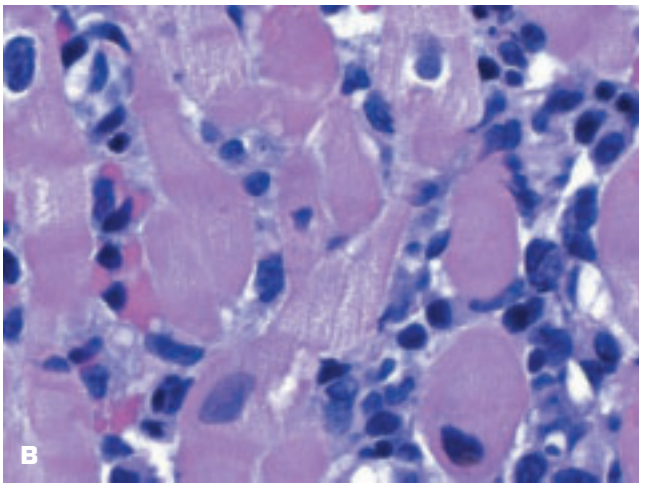

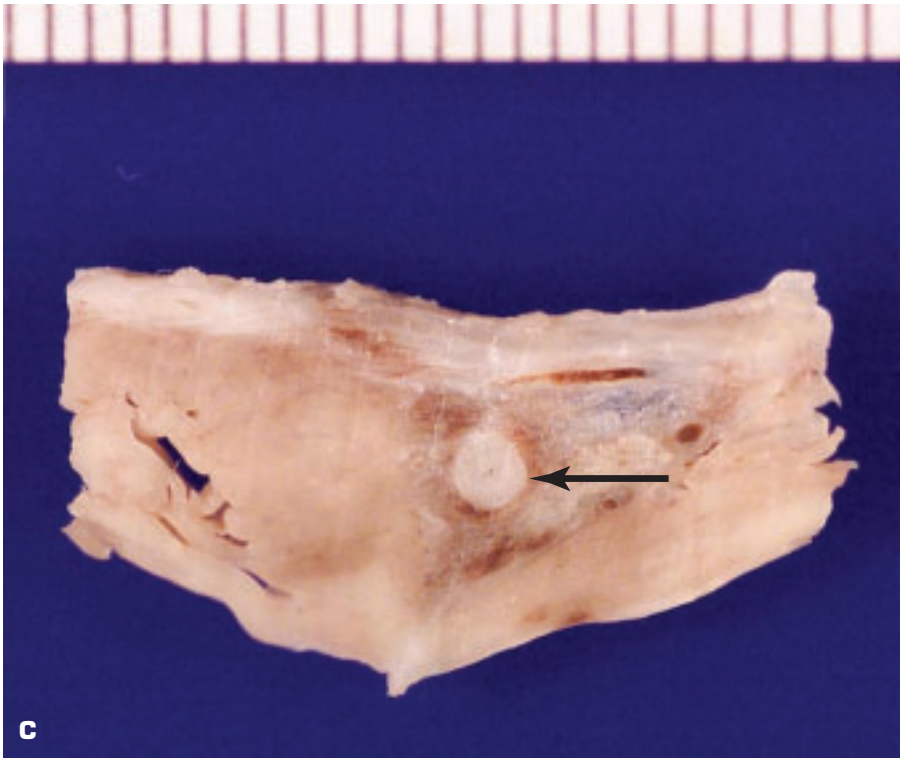

1-86. *(Continued)* **C.** Macroscopic appearance of greatly thickened donor heart coronary artery (arrow) with pinhole lumen due to graft arteriopathy (chronic rejection). **D.** Histology of the same artery showing marked intimal fibrous thickening, residual arteritis, and medial hyalinization.